NAVAL POSTGRADUATE SCHOOL
Monterey, California

THESIS

INFRARED BACKGROUND AND TARGET MEASUREMENT

by

Alexander Manolopoulos

December 1985

Thesis advisor: A. W. Cooper

Approved for public release; distribution is unlimited

URITY CLASSIFICATION OF THIS PAGE

REPORT DOCUMENTATION PAGE

REPORT SECURITY CLASSIFICATION UNCLASSIFIED	1b. RESTRICTIVE MARKINGS
SECURITY CLASSIFICATION AUTHORITY	3. DISTRIBUTION / AVAILABILITY OF REPORT Approved for public release; distribution is unlimited
DECLASSIFICATION / DOWNGRADING SCHEDULE	
ERFORMING ORGANIZATION REPORT NUMBER(S)	5. MONITORING ORGANIZATION REPORT NUMBER(S)
NAME OF PERFORMING ORGANIZATION val Postgraduate School	6b. OFFICE SYMBOL (If applicable) 61
	7a. NAME OF MONITORING ORGANIZATION Naval Postgraduate School
ADDRESS (City, State, and ZIP Code) Monterey, California 93943-5100	7b. ADDRESS (City, State, and ZIP Code) Monterey, California 93943-5100
NAME OF FUNDING / SPONSORING ORGANIZATION	8b. OFFICE SYMBOL (If applicable)
	9. PROCUREMENT INSTRUMENT IDENTIFICATION NUMBER
ADDRESS (City, State, and ZIP Code)	10. SOURCE OF FUNDING NUMBERS

PROGRAM ELEMENT NO.	PROJECT NO.	TASK NO.	WORK UNIT ACCESSION NO.

TITLE (Include Security Classification)
INFRARED BACKGROUND AND TARGET MEASUREMENT

PERSONAL AUTHOR(S) Manolopoulos, Alexander

TYPE OF REPORT	13b. TIME COVERED	14. DATE OF REPORT (Year, Month, Day)	15. PAGE COUNT
Master's Thesis	FROM _____ TO _____	1985 December	98

SUPPLEMENTARY NOTATION

COSATI CODES		
FIELD	GROUP	SUB-GROUP

18. SUBJECT TERMS (Continue on reverse if necessary and identify by block number)
Infrared Measurement, Background Radiance Cloud Radiance, Building Radiance, AGA

ABSTRACT (Continue on reverse if necessary and identify by block number)

The present work describes measurements of IR background radiance . To provide background radiance values for the development of the AN / SAR - 8 (IRSTD) system, the radiance of clouds and buildings was measured using the AGA Thermovision 780 . The measurement values given in Isotherm Units (photon flux equivalent) were translated into radiance values ($W/cm^2 sr$) . The emissivity of the different objects was also computed for the 8-14 μm window assuming that their emissivity in the 3-5.6 μm band is close to that of a blackbody . The average radiance of clouds was found to be 3.302×10^{-4} $W/cm^2 sr$ in the 3-5.6 μm window and 3.544×10^{-3} $W/cm^2 sr$ in the 8-14 μm

DISTRIBUTION / AVAILABILITY OF ABSTRACT	21. ABSTRACT SECURITY CLASSIFICATION
☒ UNCLASSIFIED/UNLIMITED ☐ SAME AS RPT. ☐ DTIC USERS	unclassified

NAME OF RESPONSIBLE INDIVIDUAL	22b. TELEPHONE (Include Area Code)	22c. OFFICE SYMBOL
A.W. Cooper	(408) 646 2452	61Cr

FORM 1473, 84 MAR 83 APR edition may be used until exhausted. All other editions are obsolete.

SECURITY CLASSIFICATION OF THIS PAGE

Block 20 Contd.

window . The corresponding values for buildings were 3.587×10^{-4} W/cm^{2}sr and 4.552×10^{-3} W/cm^{2}sr respectively.

Infrared Background and Target Measurement

by

Alexander Manolopoulos
Lieutenant, Hellenic Navy
B.S., Hellenic Naval Academy, 1976

Submitted in partial fulfillment of the
requirements for the degree of

MASTER OF SCIENCE IN ENGINEERING SCIENCE

from the

NAVAL POSTGRADUATE SCHOOL
December 1985

ABSTRACT

The present work describes measurements of IR background radiance . To provide background radiance values for the development of the AN / SAR - 8 (IRSTD) system, the radiance of clouds and buildings was measured using the AGA Thermovision 780 . The measurement values given in Isotherm Units (photon flux equivalent) were translated into radiance values (W/cm^2sr) . The emissivity of the different objects was also computed for the 8-14 μm window assuming that their emissivity in the 3-5.6 μm band is close to that of a blackbody . The average radiance of clouds was found to be 3.302×10^{-4} W/cm^2sr in the 3-5.6 μm window and 3.544×10^{-3} W/cm^2sr in the 8-14 μm window . The corresponding values for buildings were 3.587×10^{-4} W/cm^2sr and 4.552×10^{-3} W/cm^2sr respectively.

TABLE OF CONTENTS

I. INTRODUCTION 10

II. BACKGROUND TO PROBLEM 13

A. GENERAL 13

B. EFFECTS OF BACKGROUND CLUTTER IN IMAGING . . . 14

C. BACKGROUND SUPPRESSION SCHEMES 15

D. CLUTTER SUPPRESSION SCHEMES 17

E. CONCLUSION 21

III. CLOUDS,BACKGROUNDS AND THEIR SIGNATURES 22

A. CLOUDS. 22

1. Reflection of IR Radiation by Clouds . . . 25

2. Scattering of IR Radiation by Clouds . . . 25

3. Emission of IR Radiation by Clouds 32

B. BACKGROUNDS 34

1. Marine Backgrounds 34

2. Terrestrial Backgrounds 36

IV. LOWTRAN PROPAGATION / RADIANCE CODE 40

A. MODELS FOR PROPAGATION OF IR RADIATION THROUGH THE ATMOSPHERE 40

B. LOWTRAN CODE 40

C. INPUTS TO LOWTRAN 6 CODE 41

D. INPUT DATA USED 42

E. RESULTS OBTAINED 42

V. EQUIPMENT 43
A. THE AGA THERMOVISION SYSTEM 43
B. GENERAL DESCRIPTION OF THE "AGA THERMOVISION 780" 43
1. Optics and Scan Mechanism 43
2. Detectors and Cooling 45
3. Display 45
4. Technical Data 45
C. MEASUREMENT TECHNIQUES 45
D. DIRECT MEASUREMENT PROCEDURE 56
E. CORRECTION OF MEASUREMENTS FOR NON-IDEAL SITUATION 59

VI. EMPIRICAL CALIBRATION OF THE AGA 61
A. GENERAL 61
B. NEAR FIELD EXPERIMENT 61
C. FAR FIELD EXPERIMENT 63
D. CONCLUSIONS FROM THE EMPIRICAL CALIBRATION . . 67

VII. SIGNATURE MEASUREMENTS 70
A. MEASURED OBJECTS 70
B. FORMULATION OF MEASUREMENTS 71
C. APPLICATION OF THE FORMULATION TO THE EXPERIMENTAL DATA 78
D. SAMPLE CALCULATION 79

VIII. DATA ANALYSIS , PRESENTATION OF RESULTS 82

A. DATA ANALYSIS 82

1. Emissivity 82

2. Calculation of the Emissivity in the LW . 83

3. Comments 84

B. PRESENTATION OF RESULTS 86

IX. CONCLUSIONS , RECOMMENDATIONS 91

A. CONCLUSIONS 91

B. RECOMMENDATIONS 91

APPENDIX A TI-59 PROGRAM FOR CALCULATION OF THE IN-BAND FLUX 93

LIST OF REFERENCES 96

INITIAL DISTRIBUTION LIST 97

LIST OF TABLES

1. AGA SENSOR TECHNICAL INFORMATION. 46

2. NEAR FIELD MEASUREMENTS 66

3. FAR FIELD MEASUREMENTS 68

4. DATA COLLECTED 87

5. LOWTRAN OUTPUT 88

6. RADIANCE OF MEASURED OBJECTS 89

7. AVERAGE RADIANCE VALUES 90

ACKNOWLEDGEMENTS

The present THESIS was carried out under the sponsorship of SPAWARSYSCOM , PDW107-3 .

The author would like to express his sincere appreciation to many people whose help for the completion of this project was great.

The assistance of Bob Sanders and Professor E.C. Crittenden was much appreciated . The guidance of Professor A. W. Cooper insured that the present work is complete .

Finally , a special note of thanks is given to my wife Anna-Christina without whose help and support , the completion of the present work would have been impossible , and to my son Theodoros whose smile gave me courage to continue on whenever problems were encountered.

I. INTRODUCTION

An important element in Naval Warfare Defence is the development of a surveillance system capable of monitoring the appearance and progress of any potential threat. The infrared (IR) spectral region shows good promise for passive detection systems able to detect a variety of targets at different altitudes. Such a system is the Infrared Search and Target Designation (IRSTD) System (AN/ SAR-8) currently in engineering development.

In support of the development of such a system, it is necessary to fully specify and understand the IR radiance from the earth - atmosphere scene within a given field-of-view (FOV). Detecting a target by its radiation requires that not only the target intensity but also the spectral and spatial structure of the background be fully understood.

Important inputs to the design of successful detection systems are recorded magnitudes and variations in the radiance from various scenes. This information will help in developing data processing algorithms to distinguish radiation signatures of clouds and other surfaces from those of the target.

In the context of this THESIS , data on cloud and background radiance were collected and analyzed for the

purpose of later development of algorithms that will aid the AN/SAR-8 to ignore false targets generated by background , atmospheric or non atmospheric, IR radiation.

These data were collected using the " AGA 780 Thermovision", a liquid nitrogen cooled thermographic device able to detect IR radiation in the Middle IR, called hereafter Short Wave - SW (3-5.6 micrometers) , and in the Far IR , called hereafter Long Wave - LW (8-14 micrometers).

The present work consists of eight chapters following the introduction . The first chapter describes the problem and the expected output of the work. In the second chapter a theoretical overview is presented , along with data from the literature , of clouds and different backgrounds. The third chapter describes how the LOWTRAN propagation / radiance code was used to give transmittance of the atmosphere under the various circumstances of the measurements. The fourth chapter lists the capabilities of the AGA equipment and the mode of operation used . The fifth chapter describes how the AGA was calibrated empirically . In the sixth chapter the method which was actually used is presented both mathematically and analytically . In the seventh chapter measured cloud and background signatures are listed, analyzed and presented as final results. The last chapter consists of the

conclusions that the results lead to and suggestions for possible improvements and future work in the area.

The results obtained are not expected to have significant quantitative importance , due to the wide variety of possible background radiators and meteorological conditions , but it is hoped that they will provide a starting point for further work on the subject.

II. BACKGROUND TO PROBLEM

A. GENERAL

All objects in our environment , either cold or hot, radiate IR energy detectable by the IRSTD system.

The IRSTD , as mentioned before , should be capable of determining whether an observed IR source is (1) an airplane/ missile , or (2) an unwanted source such as clouds, birds, or shore features.

There are several atmospheric and terrain conditions affecting the translation of emitted radiation into meaningful signal. Two of the most important factors are the atmospheric background and the atmospheric absorption.

Atmospheric background consists mainly of clouds, rain, snow, clear sky etc. Terrestrial background consists of land, mountains, hills, cities, buildings etc.

Here we will deal with cloud and building signatures. The radiance of a selection of such sources was measured using the "AGA 780" system.

The equipment used is designed to provide the temperature of an object if its emissivity is known or vice versa. An empirical calibration of the "AGA 780" along with the application of some simple mathematical formulae was needed in order to obtain radiance measurements.

The second factor mentioned above , the atmospheric absorption, has been dealt with by using the LOWTRAN code for propagation of IR radiation. Specifically the LOWTRAN 6 computer program was used to provide attenuation factors under different atmospheric conditions.

B. EFFECTS OF BACKGROUND CLUTTER IN IMAGING

Background clutter is an important factor limiting the performance of thermal imaging equipment . Clutter emission from clouds , birds and terrestrial objects generates a sensor response which may either mask the signal from a target or appear as a false target .

It is impossible to predict how large spatially or how intense a clutter signal from background would be. Background clutter may consist of either emission or scattering from small objects (eg. birds) as well as from large objects (eg. clouds) [Ref. 1] .

Targets and clutter will be sensed by an imaging system as having a small temperature difference from the background, ΔT. This temperature difference can be expressed as radiation contrast C_R , as described by Lloyd [Ref. 2].

$$C_R = \frac{W_T - W_B}{W_T + W_B} \qquad \text{(II-1)}$$

W_T = target radiant emittance (W/m^2)

W_B = background radiant emittance (W/m^2)

If the total radiant emittance W(T) is

$$W(T) = \sigma T^4 \qquad \text{(Stefan's law)} \qquad \text{(II-2)}$$, then

$$\frac{\partial W(T)}{\partial T} = 4 \sigma T^3 \qquad \text{(II-3)}$$

or, $$\Delta W(T) = 4 \sigma T^4 \Delta T \qquad \text{(II-4)}$$

Now $$C_R = \frac{W_T - W_B}{W_T + W_B} \qquad \text{(II-1)}$$

For $$W_B = W(T) = \sigma T^4 \qquad \text{(II-5)}$$

and $$W_T = W(T+ \Delta T) = W(T) + \frac{\partial W(T)}{\partial T} \Delta T \qquad \text{(II-6)}$$

$$C_R = \frac{\Delta W(T)}{2W(T) + \Delta W(T)} \qquad \text{(II-7)}$$

$$= \frac{4 \sigma T^3 \Delta T}{2 \sigma T^4 + 4 \sigma T^3 \Delta T}$$

$$= \frac{2 \Delta T}{T + 2 \Delta T} \qquad \text{or,}$$

$$C_R = \frac{2 \Delta T}{T} \text{ , for small } \Delta T. \qquad \text{(II-8)}$$

For typical scenes ΔT is of order 1°K so this approximation may be justified.

C. BACKGROUND SUPPRESSION SCHEMES

A filtering system (subtraction scheme) will be needed to suppress the background signal. This could

be an automatic background suppression system that will sense the average background signal and subtract it.

A problem could arise here when the temperature of the target and its background are nearly the same (zero contrast). This will happen twice each day .

Hudson [Ref. 3] gives a very good example showing that last point. A truck is parked in an open field so that an infrared system can view it . Observations are made over a period of 24 hours and variations are found in the contrast between the vehicle and its background . In the afternoon the truck has been heated enough by the sun to be warmer than the background ,giving a positive contrast. During the early evening hours the vehicle , because of its large thermal capacity , cools more slowly than the background and the contrast is even greater (more positive) . At night the truck cools more rapidly , passes the point of equal temperature to the background and the contrast passes through zero to become negative. As the sun rises again the background warms more rapidly than the truck and the contrast becomes more negative . Later in the morning the heating of the sun will be sufficient to cause a period of zero contrast and then a positive one. That

shows that " for many targets and background combinations , there are two intervals in any 24-hour period during which the target cannot be detected because there is insufficient radiation contrast between it and its background " .

There are no good methods of eliminating this effect ; the best thing to do would be to wait until the period of "washout" passes.

D. CLUTTER SUPPRESSION SCHEMES

Assuming that targets and clutter will have different temperature from the background and that the background suppression is successful , the problem of eliminating clutter still remains.

Several unwanted signals that will have small ΔT above the background will be present . These signals can be from birds , clouds , buildings etc. . They will all appear as threshhold crossings exactly as a target could appear.

To avoid confusion caused by these signals several methods can be used . The use of each one will depend on the task that the system will perform (early warning, detection , tracking etc.) and on the kind of clutter expected (small or large , intense or not).

One method could be the use of a rotating reticle , in the equipment's image plane , to achieve space filtering . This method is described by Hudson [Ref. 3] and can be used for discrimination of small targets against large clutter like clouds in seeker or tracker systems.

Other methods will be dependent mainly on the size of the target to be detected .

For example for a small target we could divide the scan electronically into small windows (each one being equal in dimension to one Instantaneous field-of-view) and test if the target appears in more than two neighbouring windows. In figure 2.1 signals A and B will be classified as targets and signal C will be classified as clutter and discarded. This scheme will not be effective against small false targets such as birds .

For large targets (eg. ships) a useful logic method could be to check if the target appears in three out of four successive windows. In figure 2.2 signals A and B will be classified as targets but signal C will be classified as clutter. This system may perhaps not detect a small target (however , a missile may be detected since its booster is heating the air surrounding the exhaust gas , and will give a large target).

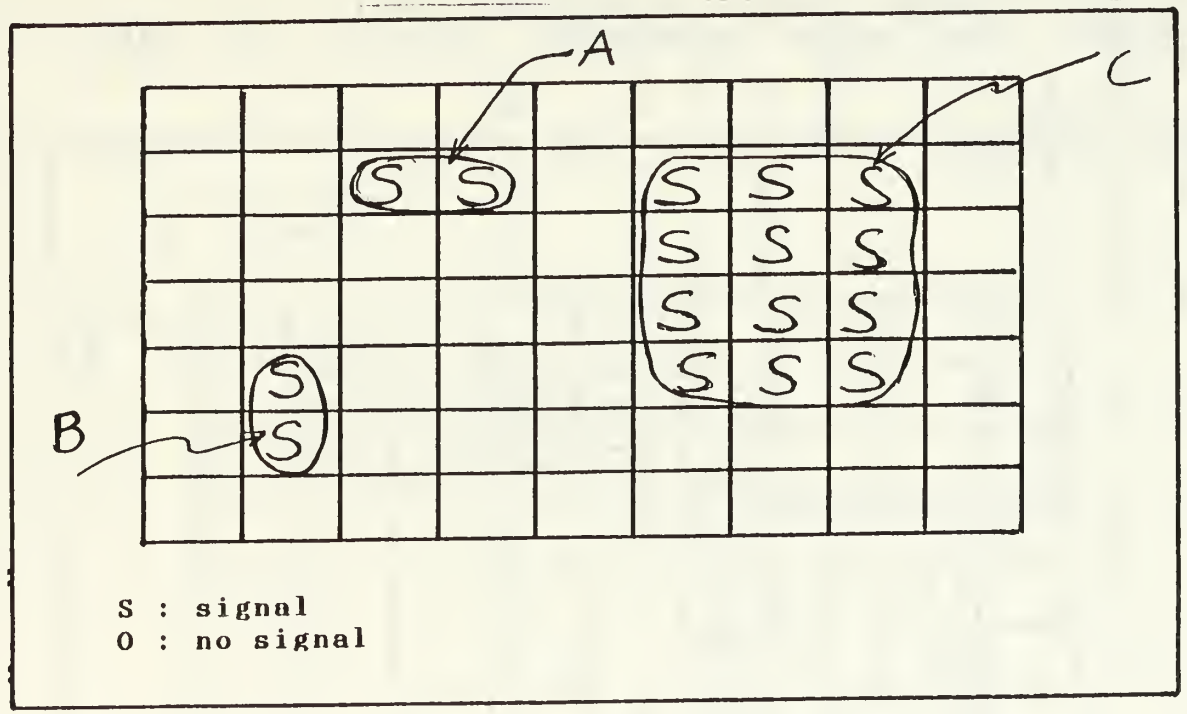

Fig. 2.1 Clutter suppression scheme for use in system that will detect small targets.

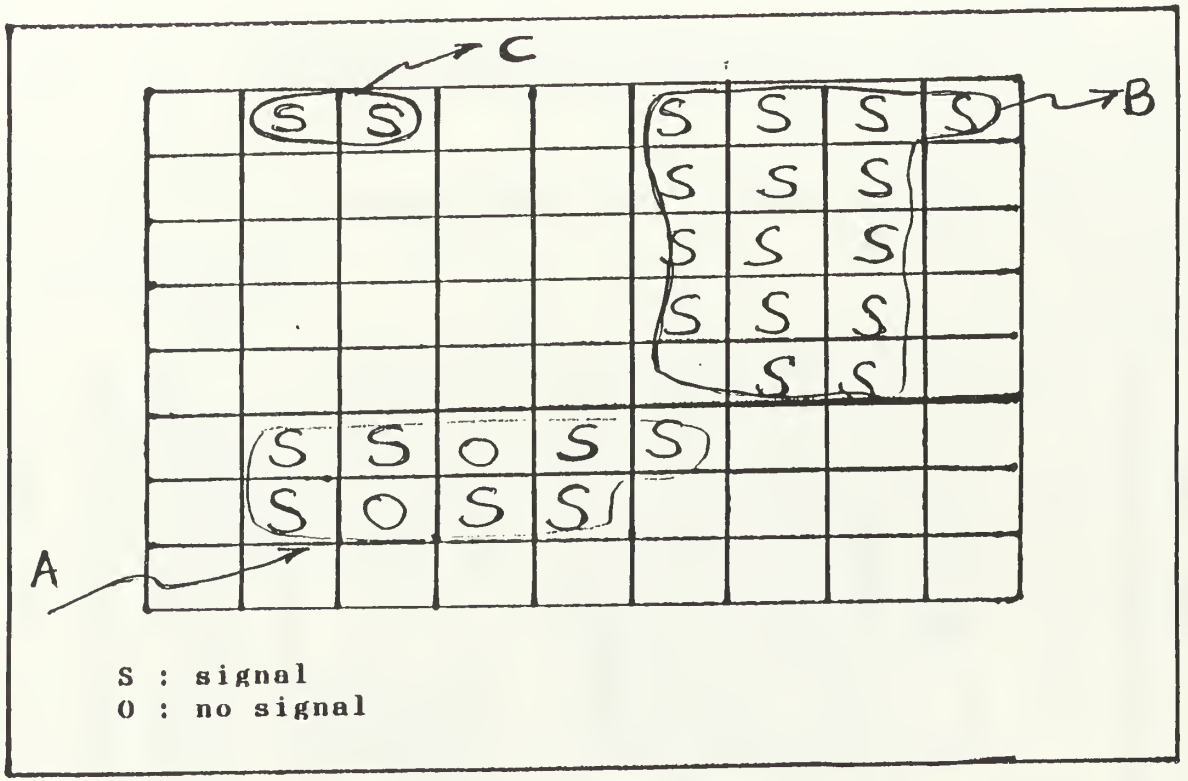

Fig. 2.2 Clutter suppression scheme for system that will detect large targets.

Other possible methods could be software analysis of the movement of the targets (eliminating for example all signals not showing any movement at the risk of discarding ships that will be stationary) , or analysis of signature patterns and statistical comparison with known signatures (although this might be very difficult due to the wide variety of clutter signatures).

E. CONCLUSION

What is obvious from the above is that it will be useful to know what amount of thermal radiation is emitted by different kinds of clutter like clouds, buildings etc. . The purpose of this THESIS is to provide and analyze thermal radiation values from such clutter.

III. CLOUDS , BACKGROUNDS AND THEIR SIGNIATURES

A. CLOUDS

Clouds are one of the main causes of undesirable IR radiation . Cloud cover in most of the regions of the world is a condition that exists about one half of the time. Figure 3.1 shows the frequency of overcast skies (curve 1) and the total frequency of overcast and partly cloudy skies (curve 2) along the 20° W Meridian, as a function of Latitude [Ref 5].

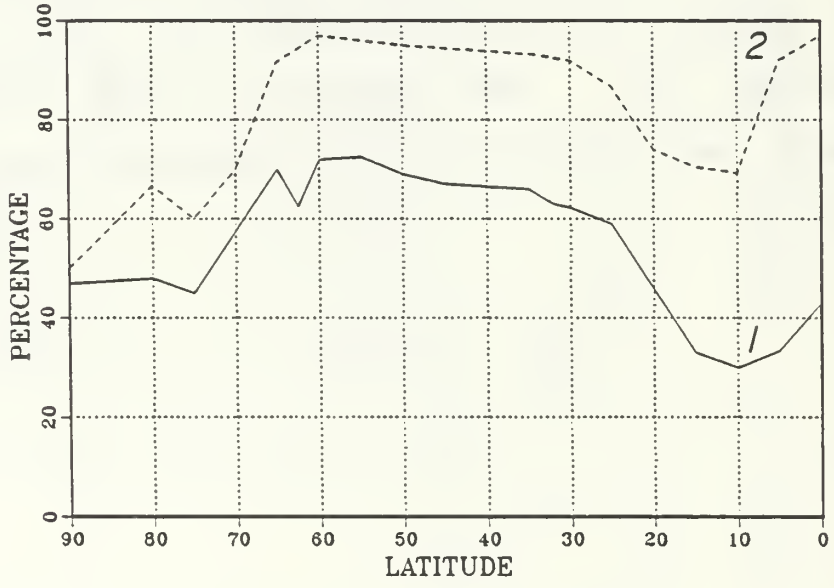

Fig. 3.1 : Latitude and dependence of frequencies of various kinds of weather along the 20° W meridian.(1) frequency of overcast skies (8-10 on a 10 fold scale for cloudiness) (2) frequency of overcast and partly cloudy (3-7) skies . Region above curve 2 characterizes frequency of clear skies.[Ref.5]

Clouds may be classified into three major categories according to the height at which they occur.

(i) High level clouds.

(ii) Middle level clouds.

(iii) Low-level clouds.

The following table shows those categories, the type of clouds in each and typical heights at which they occur.

Cloud level	Type of Clouds	Altitude at which they occur at Midlatitude. (Avg. all seasons)
High	Cirrus Cirrocumulus Cirrostratus	5 - 13 km
Middle	Altocumulus	2 - 7 km
Low	Stratocumulus Stratus	Earth's surface to 2 km

Figures 3.2 and 3.3 both from [Ref. 6] show spectral radiance from two types of clouds , Cumulus and Cirrus respectively.

Discussion of the particular behavior of each category is beyond the task of this THESIS but in general we can state that the clouds perform three things of interest in the present context:

(i) They reflect radiation originating from terrestrial objects.

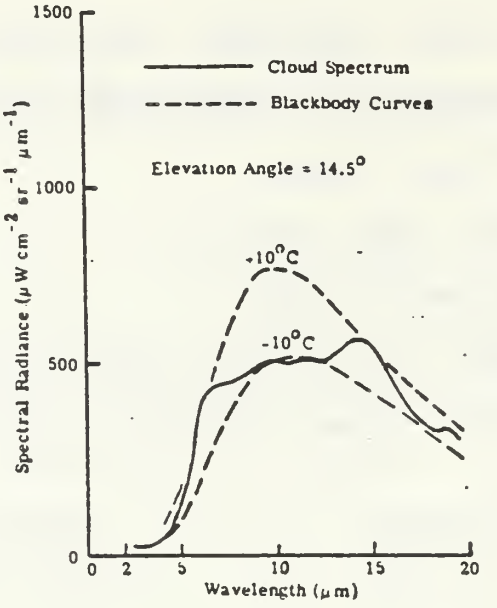

Figure 3.2 : The spectral radiance of the underside of a dark cumulus cloud . [Ref. 6]

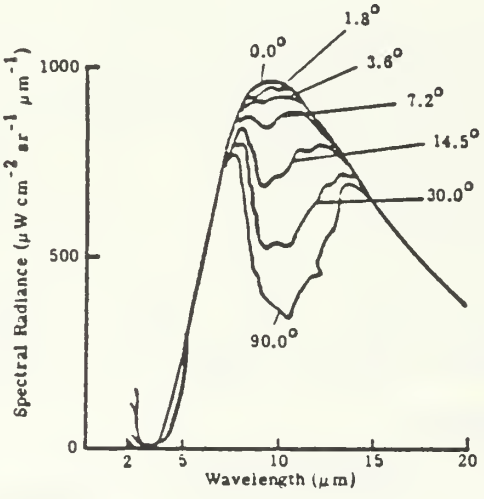

Figure 3.3 : The spectral radiance of sky covered with cirrus clouds at several angles of elevation. [Ref. 6]

(ii) They scatter solar radiation strongly , and

(iii) They emit IR radiation due to their own temperature.

Figure 3.4 [Ref. 10] shows how solar thermal radiation components reach the surface of the earth and then how they are reemitted back. There we see that of the incoming thermal radiation , 3% is absorbed by clouds and 20% is reflected by clouds back to space. On the other hand emission by clouds is responsible for 26% of the outgoing radiation to space.

1. Reflection of IR Radiation by Clouds

Clouds reflect IR radiation from terrestrial objects. Typically the reflectance of a middle layer cloud ranges from 0.75 to 0.1 in the spectral range 0.2 to 4 μm (fig. 3.5) [Ref. 6].

The reflectance of a cloud increases with the cloud thickness, and with decreasing mean free path of a light ray. It also varies with the solar zenith angle (fig. 3.6) [Ref. 6].

2. Scattering of IR Radiation by Clouds

The scattering process is the process by which particles absorb energy from an incident electromagnetic wave , from some direction , and reradiate that energy into the total solid angle centered at the particle. Scattering is a function of particle size, density and refractive index and also wavelength of incident light.

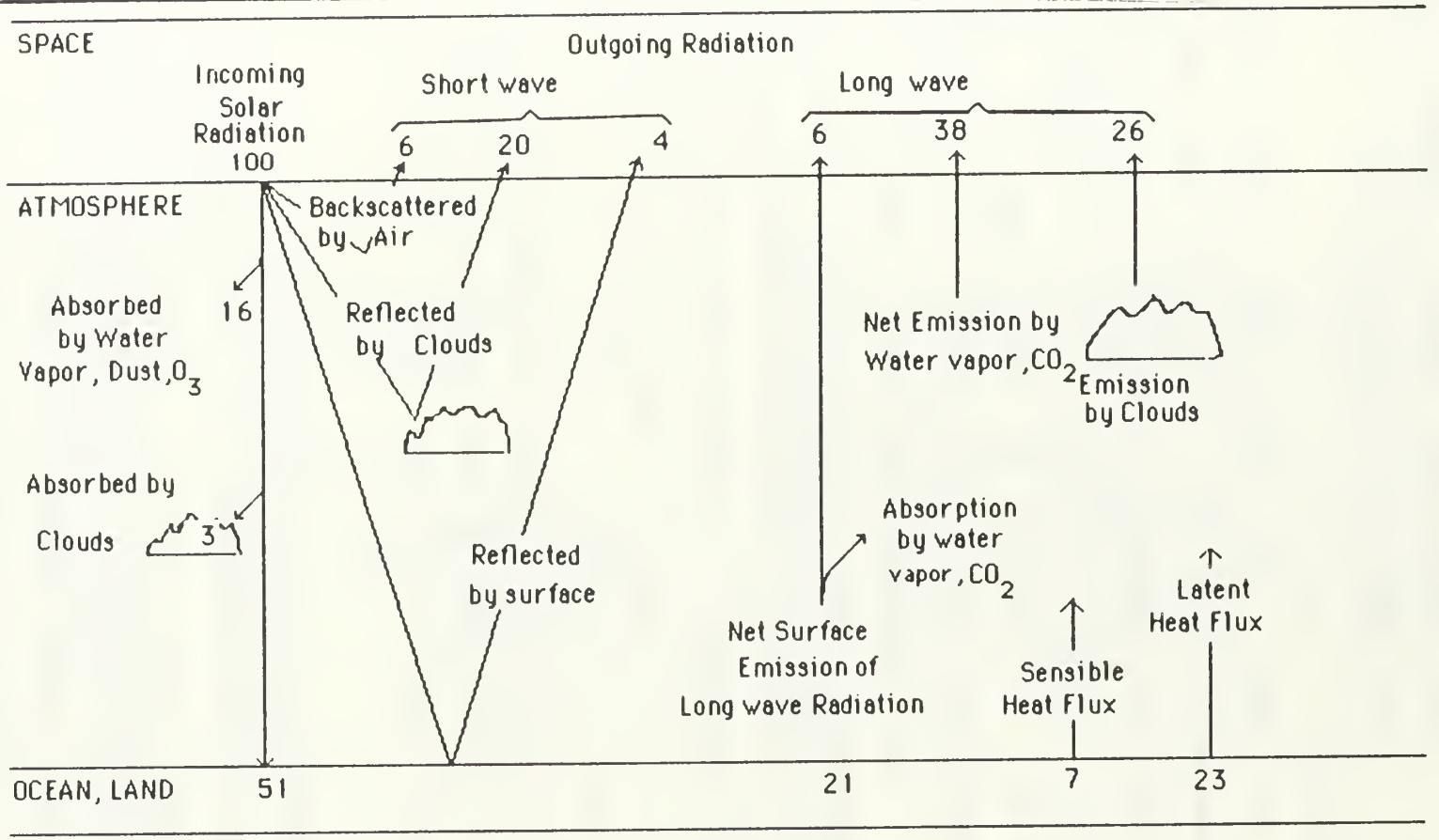

Figure 3.4 : **A summary of the solar and thermal radiation components of the Earth's Radiation budget. Numbers are percentages. [Ref. 10]**

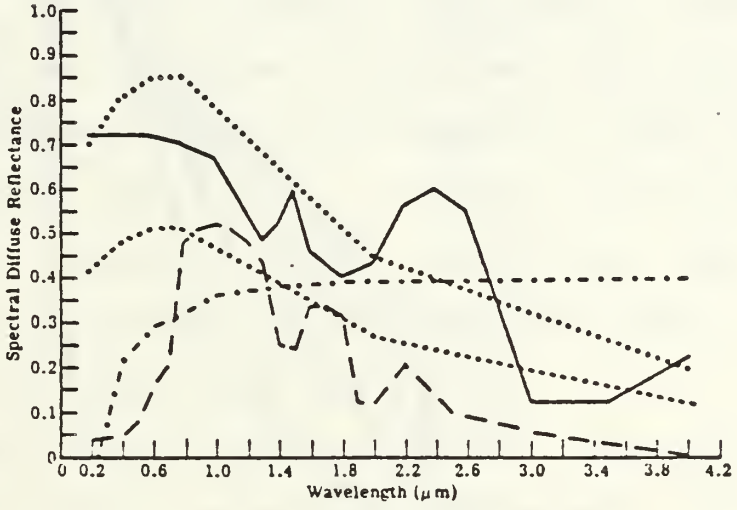

——— Clouds. Data are directional reflectance of a middle layer cloud.

••••••••• Winter Snow and Ice. Data are directional reflectance of dry snow.

•••••••••••• Summer Ice. Data are directional reflectance of summer Arctic ice.

• – • – • – Soil and Rocks. Data represent the average value of the bidirectional reflectance, ρ_λ (45°, 0, 0, 0), of gravel, wet clay, dry clay, tuff bedrock, and sandy loam.

— — — Vegetation. Data represent the average value of directional reflectance of many types of vegetation (from the ERIM Data File).

Figure 3.5 : Spectral diffuse reflectance of Earth-atmosphere constituents. [Ref. 6]

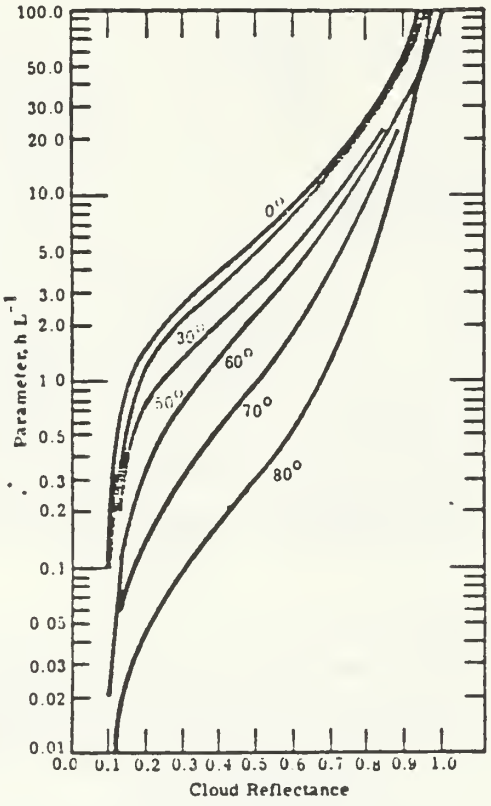

Figure 3.6 : The variation in reflectance as a function of cloud thickness parameter hL^{-1} for different solar zenith angles. The cloud thickness is h and the mean free path of a light ray is L . [Ref. 6]

Water clouds contain water-droplets and ice-crystals with radii from 1 μm to about 10 μm and concentrations of 300-10 per cm^3 . (for comparison purposes the corresponding values for raindrops are 10^2 -10^4μm and 10^{-2} - 10^{-3} per cm^3). Figure 3.7 [Ref. 11] shows the water droplet size distribution as a function of drop radius for various cloud cases. The highest clouds are composed of large ice crystals of radii greater than 50 μm. The lower clouds can be assumed to be at above freezing temperatures and therefore water droplet clouds. Figure 3.8 [Ref. 10] shows the composition of clouds vs. temperature.

Under those considerations Mie scattering (particle size comparable to wavelength) is dominant assuming that incident solar radiation at the clouds has a peak at about 0.5-1 μm and land radiation has a peak at about 10 μm. Rayleigh scattering (particle size much less than wavelength) is of less importance in connection with water clouds.

We can say that the solar scattering through clouds occurs at wavelengths shorter than 3 μm (Near IR). Middle IR is less affected by particle scattering and the Far IR is barely affected at all.

Near IR radiation exhibits strong forward scattering in clouds, but for a heavy overcast sky multiple scattering reduces this effect.

Finally , it is clear that the relative positions of sun, observer and cloud cover are of importance in

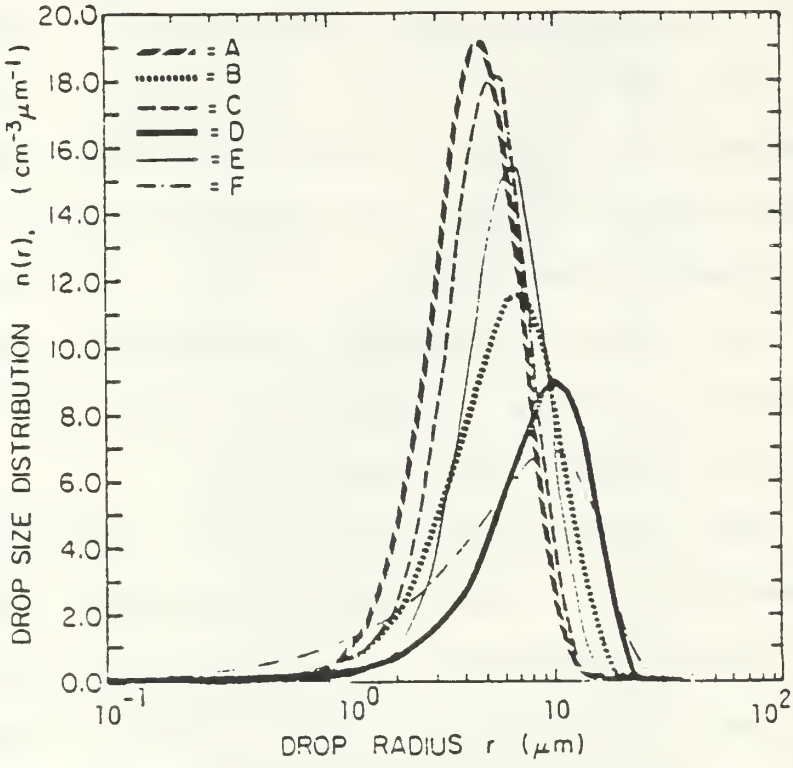

Figure 3.7 : Drop size distributions n(r) for various cloud cases.[Ref. 11]

A) stratus base
B) stratus top
C) stratocumulus base
D) stratocumulus top
E) nimbocumulus base
F) nimbocumulus top

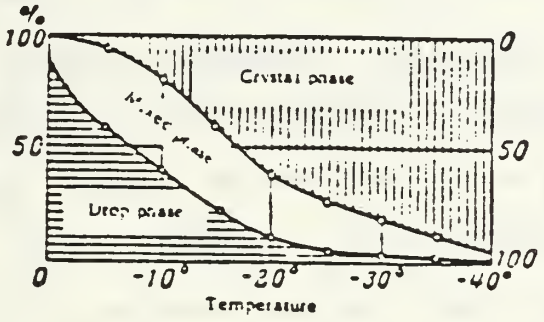

Figure 3.8 : Phase composition of clouds vs. temperature . [Ref. 10]

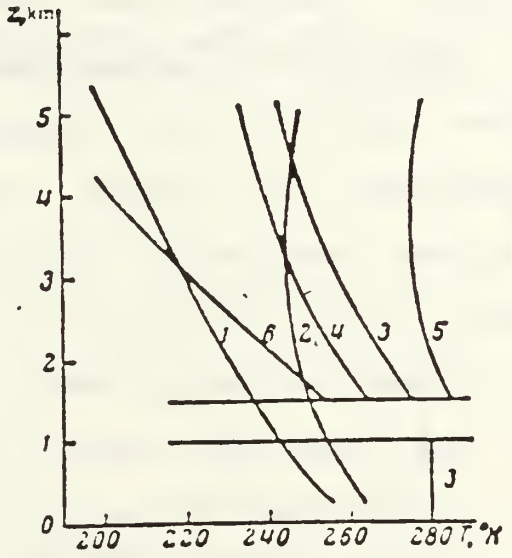

Figure 3.9 : Vertical temperature distribution for various models. [Ref. 10]

1 and 2 Cloudless atmosphere night and day

3 and 4 Cloud, night without and with scattering

5 Cloud day

6 Cloud night (selective absorber)

Note : In curves 3 and 4 the cloud is assumed to be graybody.

determining the amount of IR radiation (due to scattering) received through clouds.

3. Emission of IR Radiation by Clouds

Like all other bodies, clouds emit IR radiation due to their temperatures . Usually the temperature of a cloud differs from the surrounding air by not more than some tenths of a degree. This difference reaches a maximum of one degree for dense cumulus clouds [Ref. 10]. Under those considerations the temperature of a low cloud is about 10° C below ambient temperature at the sea surface. Also it is obvious that a cloud's temperature decreases with height. Figure 3.9 [Ref. 10] shows the vertical temperature distribution for various models of clouds .

Thick clouds (thickness>100m) ie. many free paths in thickness and clouds with content of water droplets (or ice crystals) greater than 0.5 g/cm^3 are good blackbodies [Ref. 5]. Since their temperature is of the order of 300°K they emit mainly in the 8-13 μm band. Figure 3.10 [Ref. 5] shows the spectral emissivity of cloud layers of thickness Δz and figure 3.11 [Ref. 5] shows how the integral emissivity , transmittance and absorptance varies with Δz . It is clear from that last figure that for

$\Delta z > 60m \quad \tau \dashrightarrow 0$, and

$\Delta z > 100m \quad \epsilon \dashrightarrow 1$

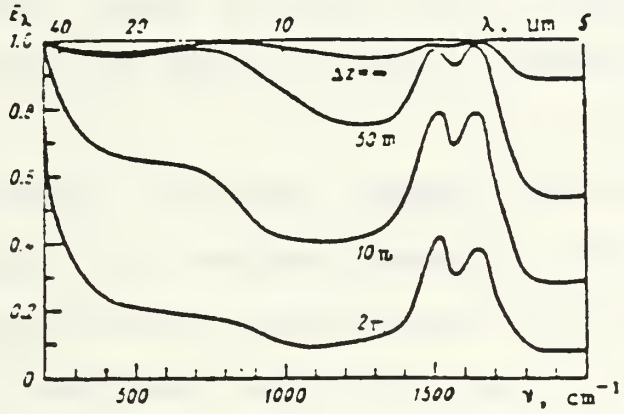

Figure 3.10 : Spectral emissivity of cloud layers of thickness Δz . [Ref. 5]

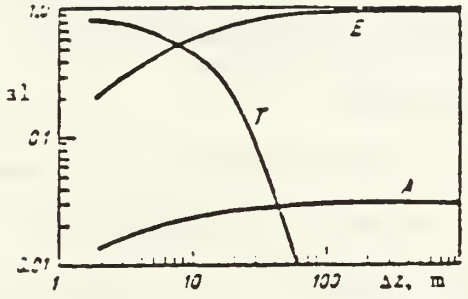

Figure 3.11 : Integral emittance (E), transmittance (T), and absorptance (A) curves. [Ref. 5]

Figure 3.12 [Ref. 6] shows the zenith sky spectral radiance from a cloud. In this figure we note two things:

(a) The large variation of the cloud spectral radiance for different ambient air temperature.

(b) That neglecting the absorption band centered at about 10 μm the cloud spectrum approaches very closely the blackbody curves of the ambient air temperature thus making the latter a very good estimate of the cloud's own temperature.

B. BACKGROUNDS

For our purpose we may consider two general categories of background (surface backgrounds).

1. Marine Backgrounds

The surface of the sea emits its own thermal radiation and also reflects incident IR radiation. The major factors that determine the amount of IR radiation due to a marine background are (1) the surface temperature of the water (2) the optical properties of the water (3) the amount of agitation of the water (4) the material properties of the bottom of the sea [Ref. 6] .

For our purpose, it has been assumed that marine backgrounds won't produce any effect by reflecting IR radiation since the reflectance of the water is less than 0.05 for angles of incidence of 50° or less as can be

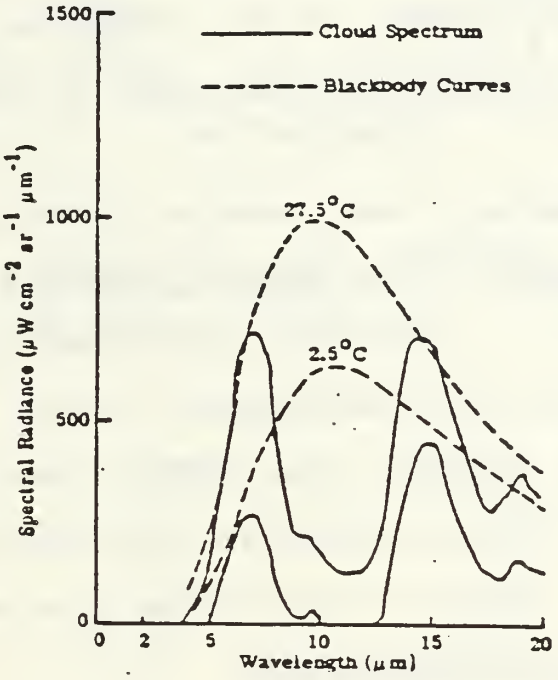

Figure 3.12 : Zenith sky spectral radiance showing the large variation with ambient air temperature. [Ref. 6]

seen in figure 3.13 [Ref. 6]. Rough sea may change that. For a Beaufort 4 wind roughened sea , for the sun at the horizon , the reflectance reaches a maximum of about 0.20 . But for the sun at an elevation of 30° or more the reflectance will be less than 0.05. (Figure 3.14 [Ref. 6])

What remains is the emission of IR radiation by the sea. The emissivity of an average rough sea is about 0.8 but the amount of IR radiation actually emitted depends on the water temperature. This temperature is near 0°C (about 4°C) in the arctic regions and 29°C near the equator. Currents may produce anomalies of several degrees Celcius as warm water flows into cold water or vice versa.

2. Terrestrial Backgrounds

Terrestrial objects have a wide variety of emissivities and temperatures. Some of them also are not opaque. Obviously the radiance of a sun heated object falls during the night when heating from the sun is absent. Figure 3.15 [Ref. 6] shows the variation in the 10 μm radiance of selected backgrounds during a 24 hour time period.

Most terrestrial objects are not blackbodies. This can be seen in figure 3.16 taken from [Ref. 6], which represents the radiance of a city on a plain (Colorado Springs) as viewed from a mountain (Pikes Peak) at a

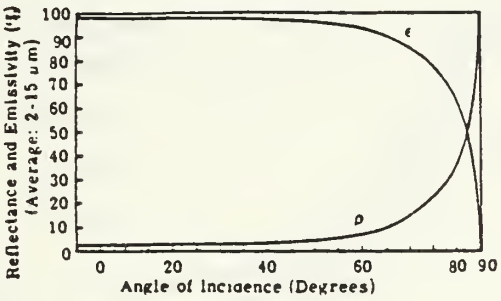

Figure 3.13 : Reflectance and emissivity of water (2 to 15 μm average) versus angle of incidence. [Ref. 6]

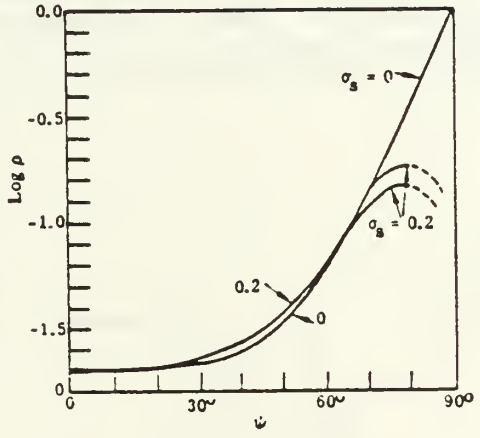

Figure 3.14 : Reflection of solar radiation from a flat surface (σ_S=0) and a surface roughened by a beaufort 4 wind (σ_S=0.2) The lower and upper branches of the curve marked σ_S=0.2 represent two assumptions regarding the effect of multiple reflection. True values are expected to lie between the indicated limits. [Ref. 6]

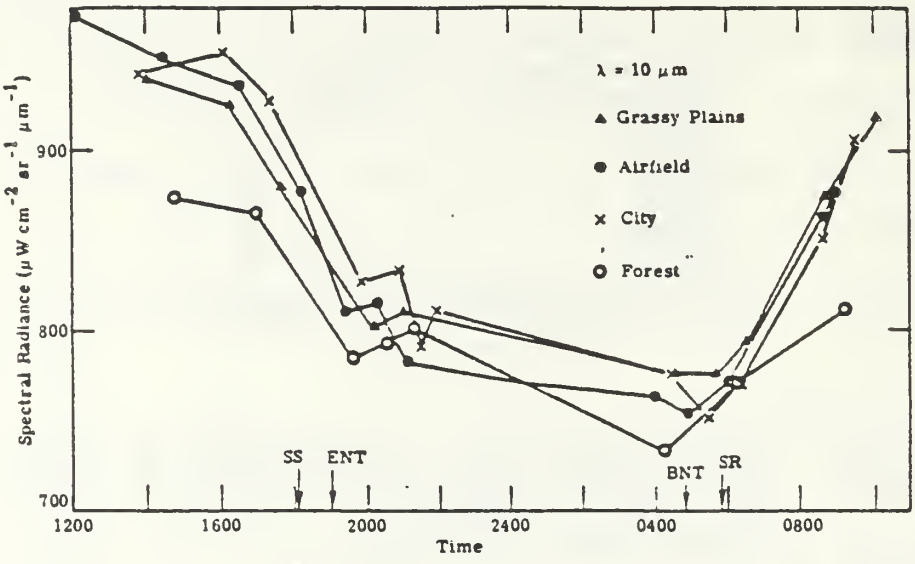

Figure 3.15 : Diurnal variation in the 10 μm Radiance of selected backgrounds . SS : sunset; ENT : end of nautical twilight; SR : sunrise; BNT : beginning of nautical twilight. [Ref. 6]

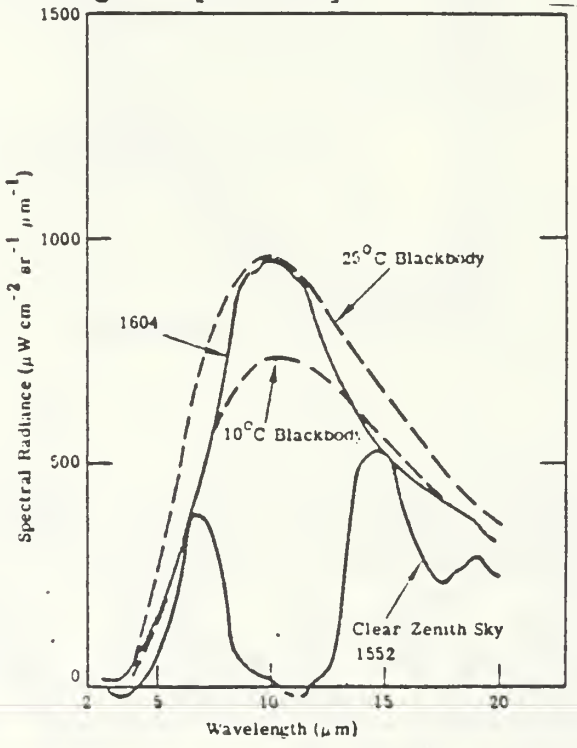

Figure 3.16 : Radiance of an urban area and clear zenith sky (Colorado Springs from Pikes Peak). [Ref. 6]

distance of about 24 km. On the other hand most of the terrestrial objects behave as graybodies .

IV. LOWTRAN PROPAGATION / RADIANCE CODE

A. MODELS FOR PROPAGATION OF IR RADIATION THROUGH THE ATMOSPHERE

For many applications , and specifically for the performance of military systems in imaging , a model which will provide accurate transmission and modification of IR radiation through an atmospheric path , and also the fluctuation in these effects is needed.

Two such models are available , the High resolution model developed by the AFCRL and the Low resolution model called LOWTRAN.

The HITRAN High Resolution models such as LASER and FASCODE are direct computation models which provide very high resolution (ie. single frequency) results. This is necessary to predict atmospheric behavior of laser radiation , but not for thermal (broad band) sources such as considered here.

B. LOWTRAN CODE

LOWTRAN has been developed as a curve-fitting program matching empirical or precomputed attenuation data . This empirical data is averaged over some specific spectral interval (20 cm^{-1}). As a consequence of the averaging over finite spectral interval, many of the rapid

spectral fluctuations of atmospheric transmittance will vanish.

Thus the LOWTRAN code can be considered as a fast but not very accurate computer program.

LOWTRAN6 , the latest version of LOWTRAN, is a program designed to calculate transmittance and/or radiance of the atmosphere for a specific set of geometrical and weather conditions , in the spectral range 0.25 to 28.57 micrometers (350 to 40,000 cm^{-1}) at 20 cm^{-1} intervals (ie. 20 cm^{-1} spectral resolution).

C. INPUTS TO LOWTRAN 6 CODE

To run LOWTRAN 6 one must specify four sets of input data (cards).

In Cards 1 & 2 one of the six available atmospheric models or a user defined set of meteorological conditions (model atmosphere) must be specified.

In Card 3 are specified the different geometrical path parameters of the problem.

In Card 4 finally are specified the spectral range over which data are required and the frequency increment at which the data are to be printed out .

D. INPUT DATA USED

This model has been used in this study to predict sky radiance and correct other radiance values for atmospheric effects.

For Card 1 the Midlatitude Winter model was used.

For Card 2 the Maritime extinction (23km visibility) model was used most of the time.

For Card 4 the wavelength bands were the 3 to 5.6 μm (3340 to 1780 cm^{-1}) and the 8 to 14 μm (1250 to 710 cm^{-1}) windows with 20 cm^{-1} spectral intervals.

Otherwise the rest of the data was dependent on the specific conditions of each measurement.

E. RESULTS OBTAINED

The program was used in its radiance mode . The average transmittance of the atmosphere and the radiance of the clear sky were recorded.

These results appear in the Table 5 of chapter eight along with the radiance values provided by the program.

V. EQUIPMENT

A. THE AGA THERMOVISION SYSTEM

"AGA Thermovision" was first introduced in 1965. The 780 System is a fourth generation development of a system which combines real time IR scanning with thermal measurement capability. By thermal measurement is meant measurement of the temperature of an object. Chapter 7 will analyze how the AGA was used to measure radiance.

The " AGA Thermovision " 780 owned by the Naval Postgraduate School (Electro-Optics Laboratory , Department of Physics) consists of a dual scanner : one channel for the 3 - 5.6 μm band (SW) and one for the 8-14 μm band (LW). It uses a two dimensional object-plane scan. Figure 5.1 shows the different components of the AGA system.

B. GENERAL DESCRIPTION OF THE "AGA THERMOVISION" 780

1. Optics and Scan Mechanism

In the AGA Thermovision 780 ,the scan is performed by two refractive prisms with eight sides. Horizontal scan lines are interlaced (with 4:1 interlace) to provide a complete frame of 400 lines. A mask at the display of the system allows 280 lines of the 400 to be viewed.

AGA Thermovision®

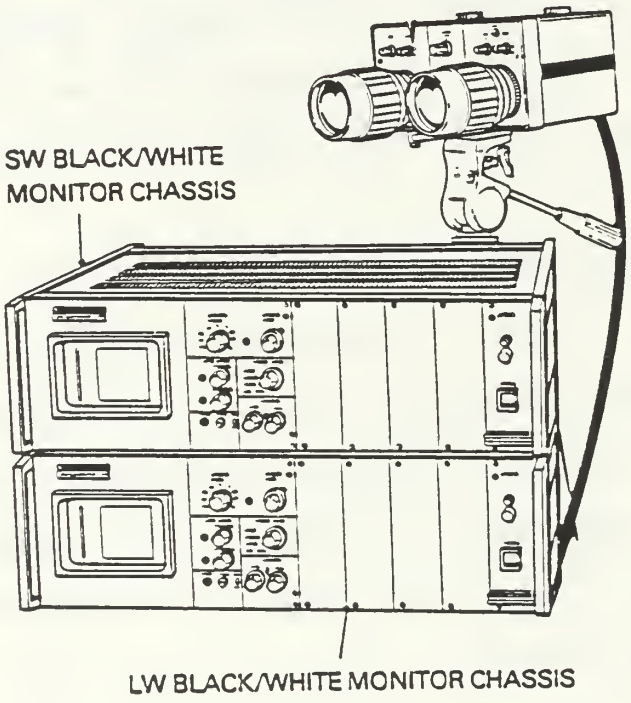

Figure 5.1 : Components of the AGA Thermovision 780. [Ref. 7]

The lenses of the SW system are constructed from silicon, and those for the LW system are constructed from germanium.

From the front of the scan head the aperture stop and the bandpass filter can be selected. For our purpose the non-filter position and the f/1.8 aperture stop have been used.

2. Detectors and Cooling

There are two detectors , both cooled to 77°K using liquid nitrogen. For SW applications an Indium-Antimonide (InSb) and for LW applications a Mercury-Cadmium-Telluride (HgCdTe) detector is used.

3. Display

A black and white display for each band gives an image of the object viewed. The brighter the object appears on the display, the more IR radiation it emits.

4. Technical Data

Technical data for the "AGA 780" appear in Table 1.

C. MEASUREMENT TECHNIQUES

The " AGA Thermovision 780" measures , as mentioned before, IR radiation within two bands (windows) or spectral ranges, the 3-5.6 μm window and the 8-14 μm window. The radiation received by the equipment includes radiation reflected by terrestrial objects in the line of

TABLE 1

AGA SENSOR TECHNICAL INFORMATION [Ref. 13]

Performance characteristics

Spectral Region (μm)	:	3 to 5.6 and/or 8 to 14 (1)
Frame rate (sec^{-1})	:	6.25
Field rate (sec^{-1})	:	25
Interlace	:	4 : 1

Replaceable Fore-Optics FOV2 (2)

FOV (deg) ,	AZ	:	7
	EL	:	7
IFOV (mrad) ,	AZ	:	1.1
	EL	:	1.1
NEΔT at 22°C (°C)		:	0.12
MDT (°C)		:	<0.1
Dynamic Range (°C)		:	-20 to 900

Optical Data FOV2 (2)

Effective Aperture Area (cm^2)	:	24
Diameter of Aperture (cm)	:	5.5
Effective Focal Length (cm)	:	9.9
f/ number	:	1.8

Detector and Cooler Data

Type and Material	:	InSb or HgCdTe
Number of Elements	:	1
Peak Wavelength (μm)	:	5 or 10

Notes: (1) According to [Ref. 13] the SW window is 2 to 5.6 μm but [Ref. 7] gives 3 to 5.6 μm.
(2) There are four other possible FOV's (3.5X3.5, 12X12,20X20,40X40) but data is presented only for the one used.

sight and also is affected by atmospheric absorption , thus making the relation to the temperature of the objects observed a non linear one.

The equipment measures the received IR radiation in " Isotherm Units (IU) " , an arbitrary unit of measurement. The value obtained has a linear relationship with received photon flux (photons/second).

If object temperature is desired , the non-linear relation of IU and Temperature (C) is given by calibration curves (SW figures 5.2 to 5.5 ,LW figures 5.6 to 5.9). In these curves the object surface emissivity has been assumed equal to one (ϵ =1 , object:black body), and no atmospheric absorption has been considered. If the object is not a black body ,or atmospheric absorption has to be taken into account, corrections have to be applied (See section V.E : Corrections of measurements for non-ideal situation).

There are two basic methods of thermal measurement using the AGA 780 :

(i) The Direct measurement where the equipment is used to obtain directly the temperature of the object without any reference to any other source of radiation.

(ii) The Relative measurement where the equipment is used to obtain temperature by comparing the radiation received from the observed object and the radiation

AGA

AGA Infrared Systems AB

INDIVIDUAL CALIBRATION OF 780 DUAL BBAR

SERIAL NUMBERS

SCANNER : SWDB 4011
DETECTOR : G 1739
FILTER : NOF
LENS : 7 3009

CALIBRATION CONDITIONS:

AMBIENT TEMPERATURE : 23 C
RELATIVE HUMIDITY : 50 %
OBJECTIVE DISTANCE : 1.0 m
CALIBRATION DATE : 82-09-17
OPERATOR : B.A

CALIBRATION CURVE CONSTANTS

APERTURE	A	B	C
1.8	811203	3117.74	1.00
2.5	449342	3127.50	1.00
3.6	267514	3161.13	1.00
5.1	161958	3182.86	1.00
7.2	96669	3220.95	1.00
10	65232	3242.19	1.00
14	38173	3253.91	1.00
20	30288	3405.76	1.00

Figure 5.2 : SW calibration curves for the AGA 780. [Ref.7]

The curves that follow are of the form

$$I = \frac{A}{C \; e^{B/T} - 1}$$

A, B, C are the empirical constants above.

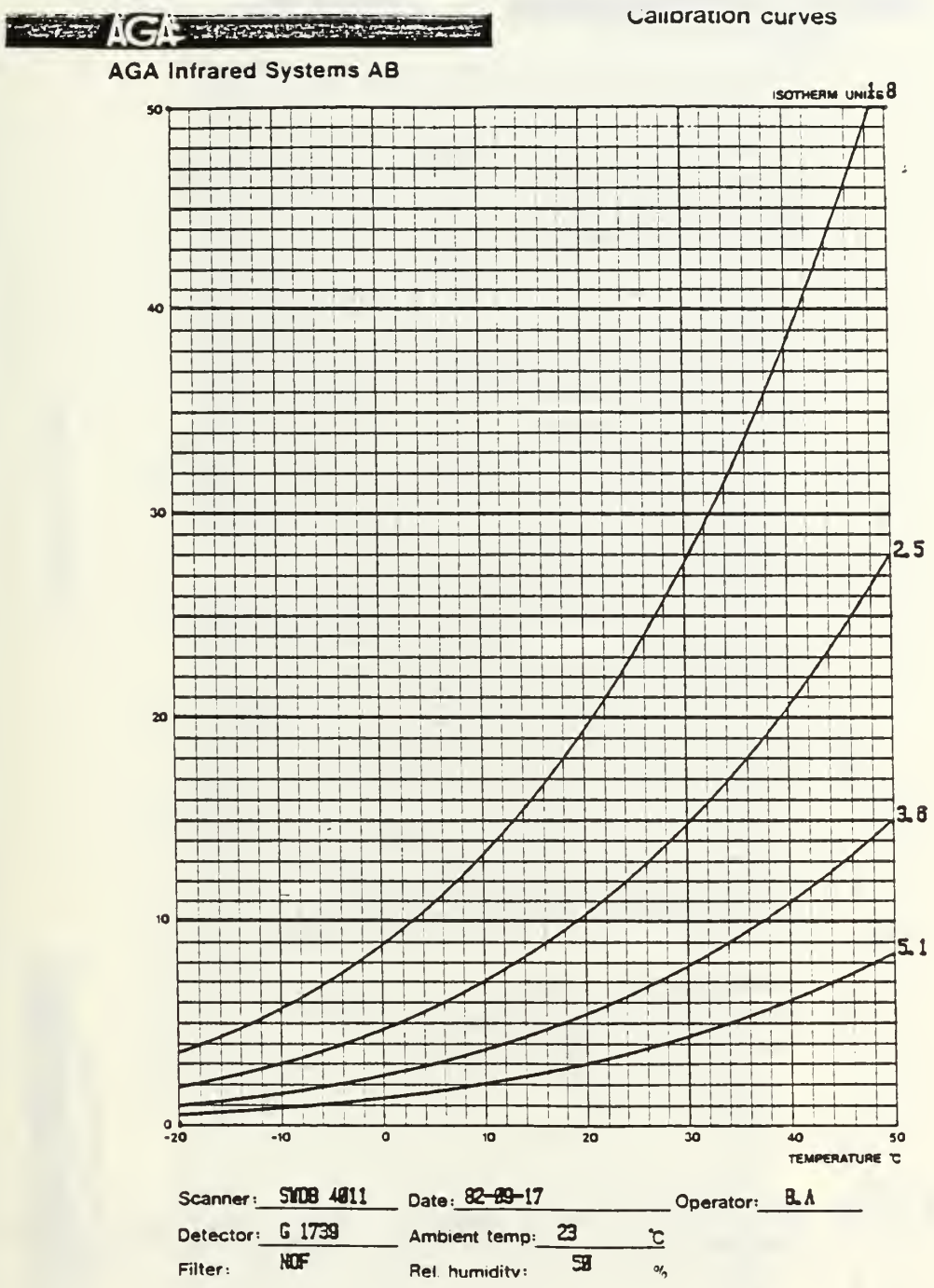

Figure 5.3 : SW calibration curves for the AGA 780. Temperature range from -20°C to 50°C. [Ref. 7]

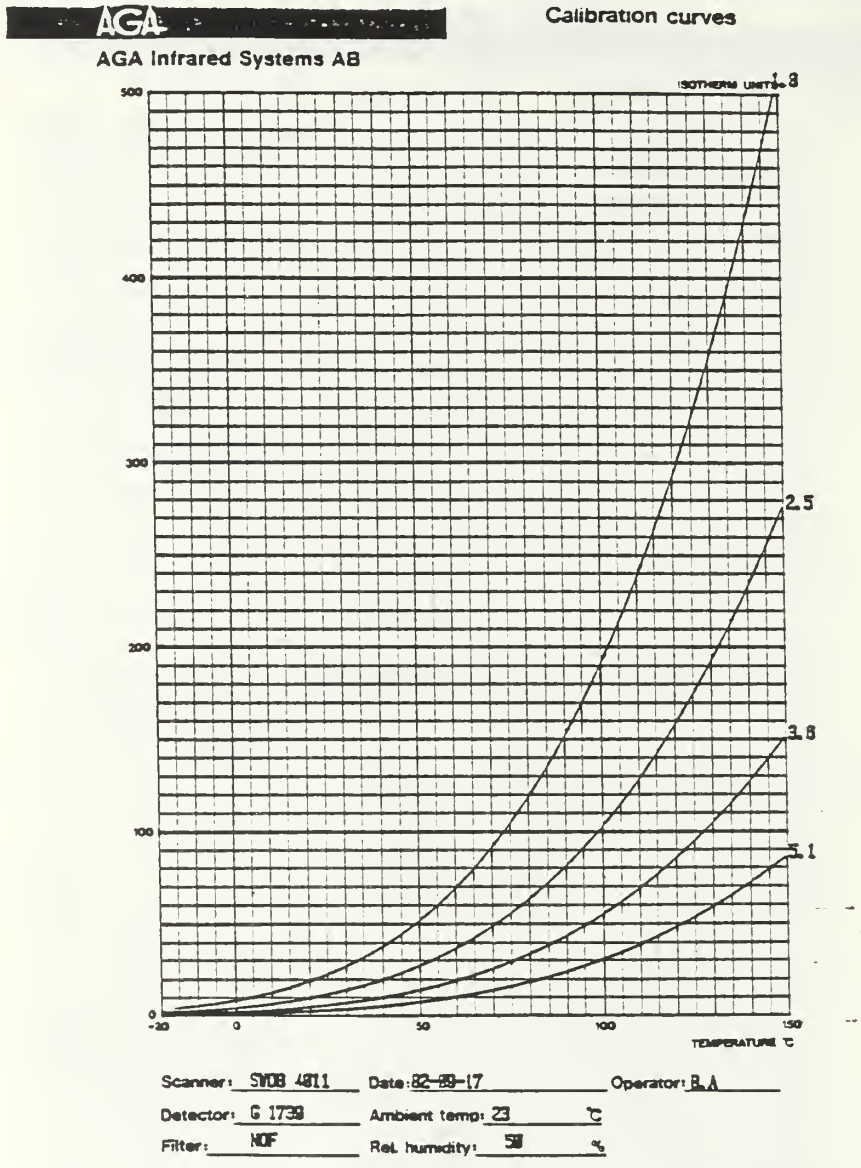

Figure 5.4 : SW calibration curves for the AGA 780. Temperature range from -20°C to 150°C. [Ref. 7]

AGA

AGA Infrared Systems AB

Calibration curves

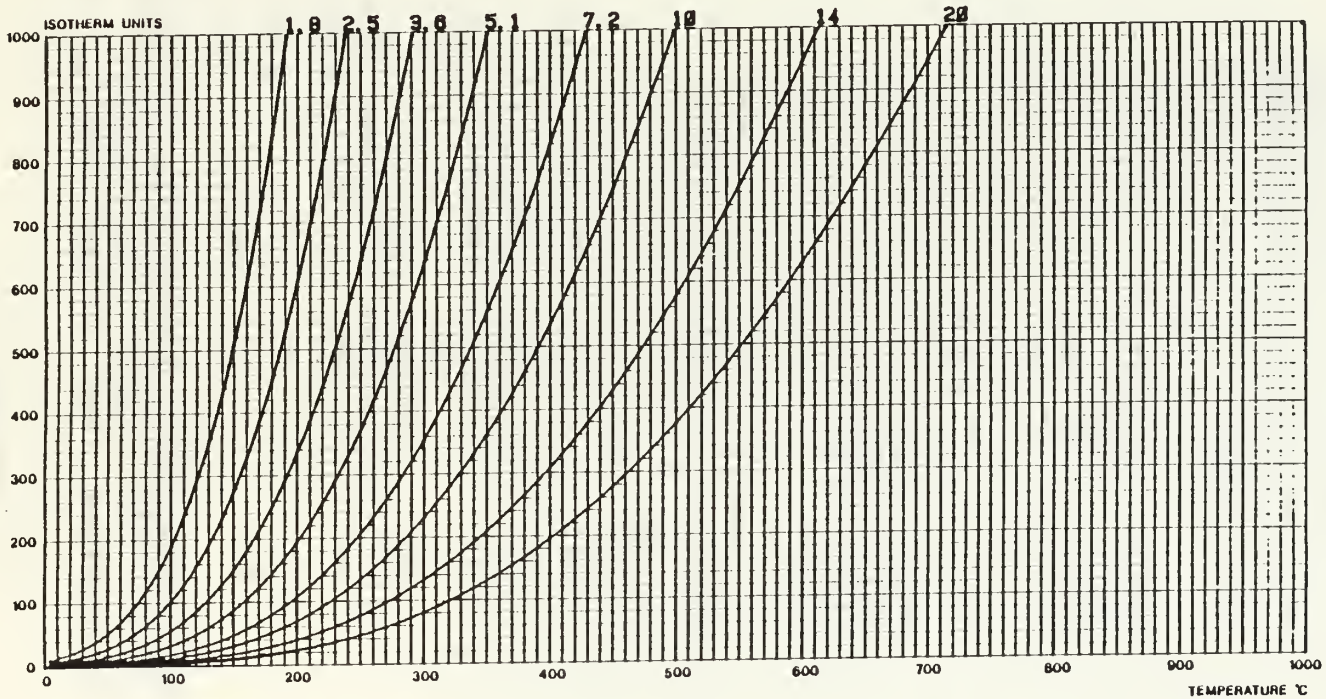

Scanner: SWDB 4011 Filter: NOF Date: 82-00-17 Rel. humidity: 50 % Operator: B.A

Detector: G 1739 Lens: 7 9000 Ambient temp.: 23 °C Object distance: 1.0 m

556 55

Figure 5.5 : SW calibration curves for the AGA 780. Temperature range from 0°C to 1000°C. [Ref. 7]

AGA

AGA Infrared Systems AB

INDIVIDUAL CALIBRATION OF 780 DUAL BBAR

SERIAL NUMBERS

SCANNER : LWDB 4011
DETECTOR : G 1739
FILTER : NOF
LENS : 7 3105

CALIBRATION CONDITIONS:

AMBIENT TEMPERATURE : 24 C
RELATIVE HUMIDITY : 55 %
OBJECTIVE DISTANCE : 1.0 m
CALIBRATION DATE : 82-09-27
OPERATOR : B.A

CALIBRATION CURVE CONSTANTS

APERTURE	A	B	C
1.8	-3581	1506.49	-0.436
2.5	-4060	1569.30	-0.759
3.6	-6514	1629.70	-1.824
5.1	5420	1610.70	2.796
7.2	1123	1606.54	1.098
10	584	1604.29	0.885
14	306	1610.60	0.773
20	195	1650.51	0.767

Figure 5.6 : LW calibration curves for the AGA 780. [Ref.7]

The curves that follow are of the form

$$I = \frac{A}{C\, e^{B/T} - 1}$$

A, B, C are the empirical constants above.

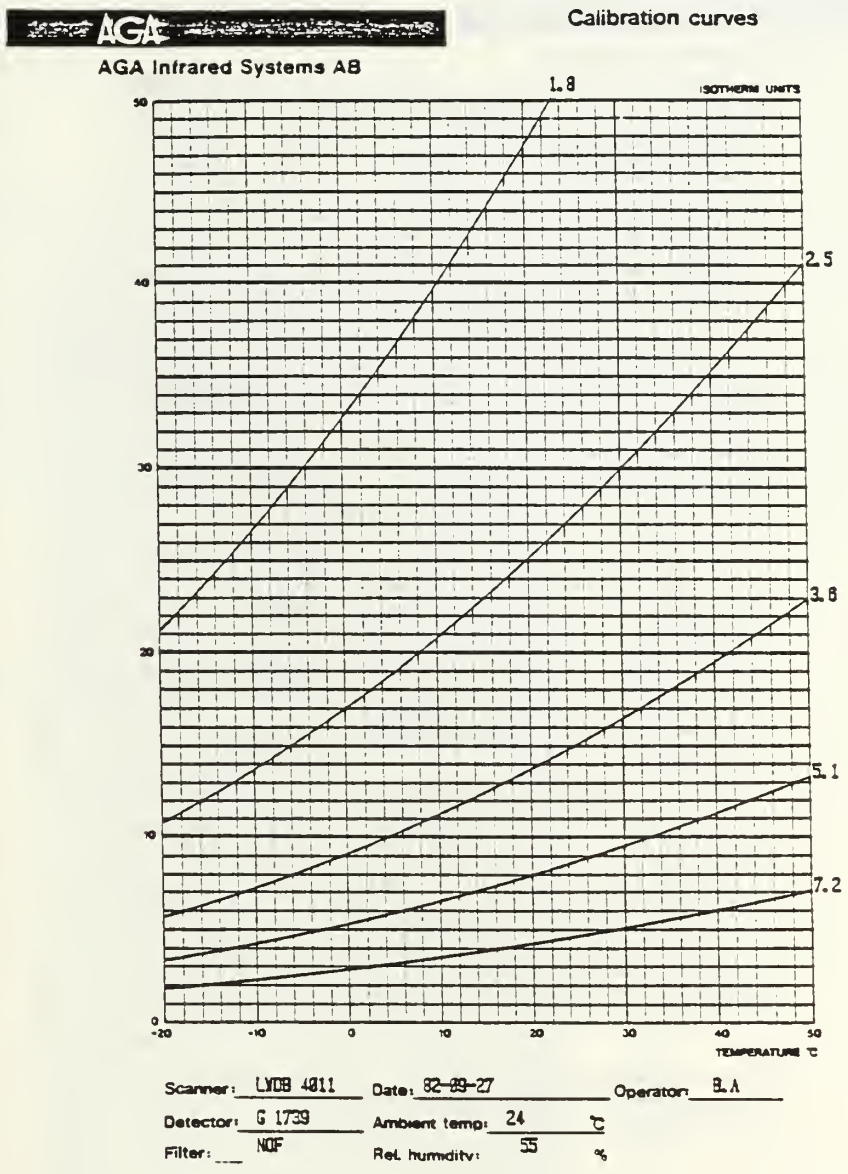

Figure 5.7 : LW calibration cuves for the AGA 780. Temperature range from -20°C to 50°C. [Ref. 7]

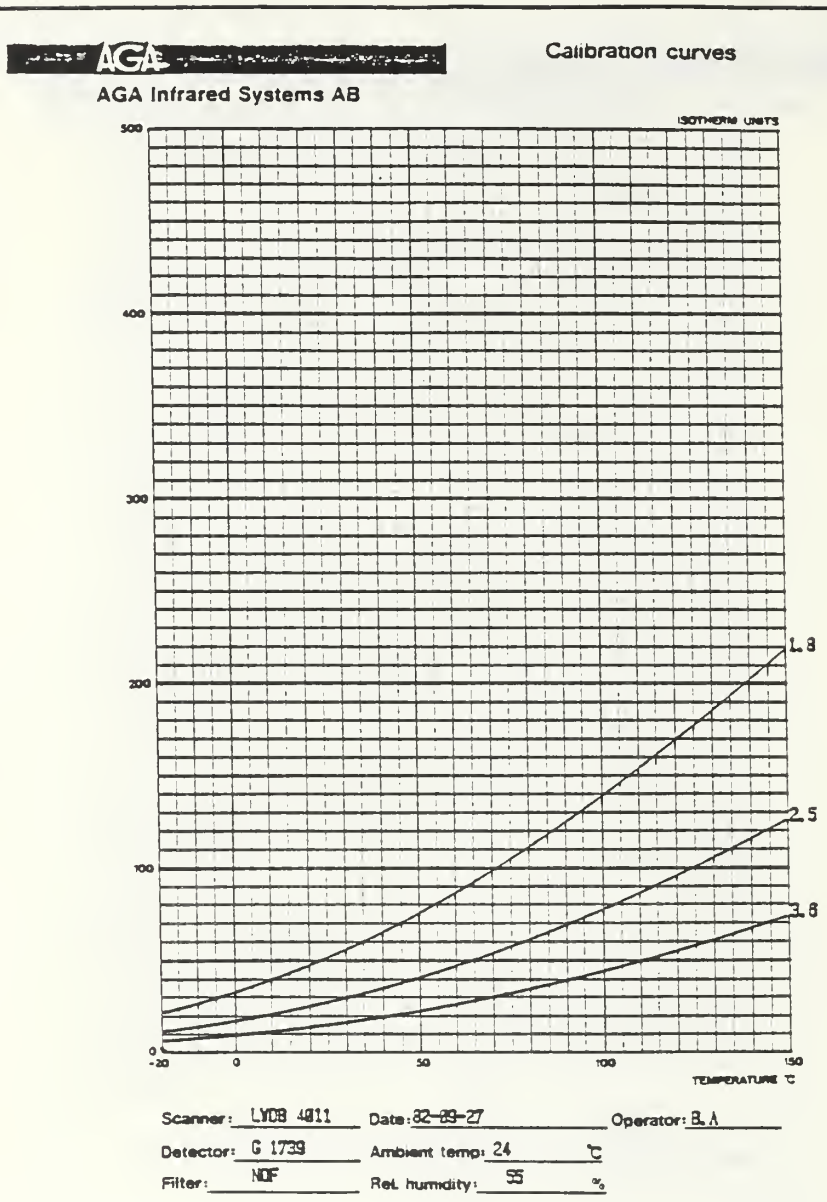

Figure 5.8 : LW calibration curves for the AGA 780. Temperature range from -20°C to 150°C. [Ref. 7]

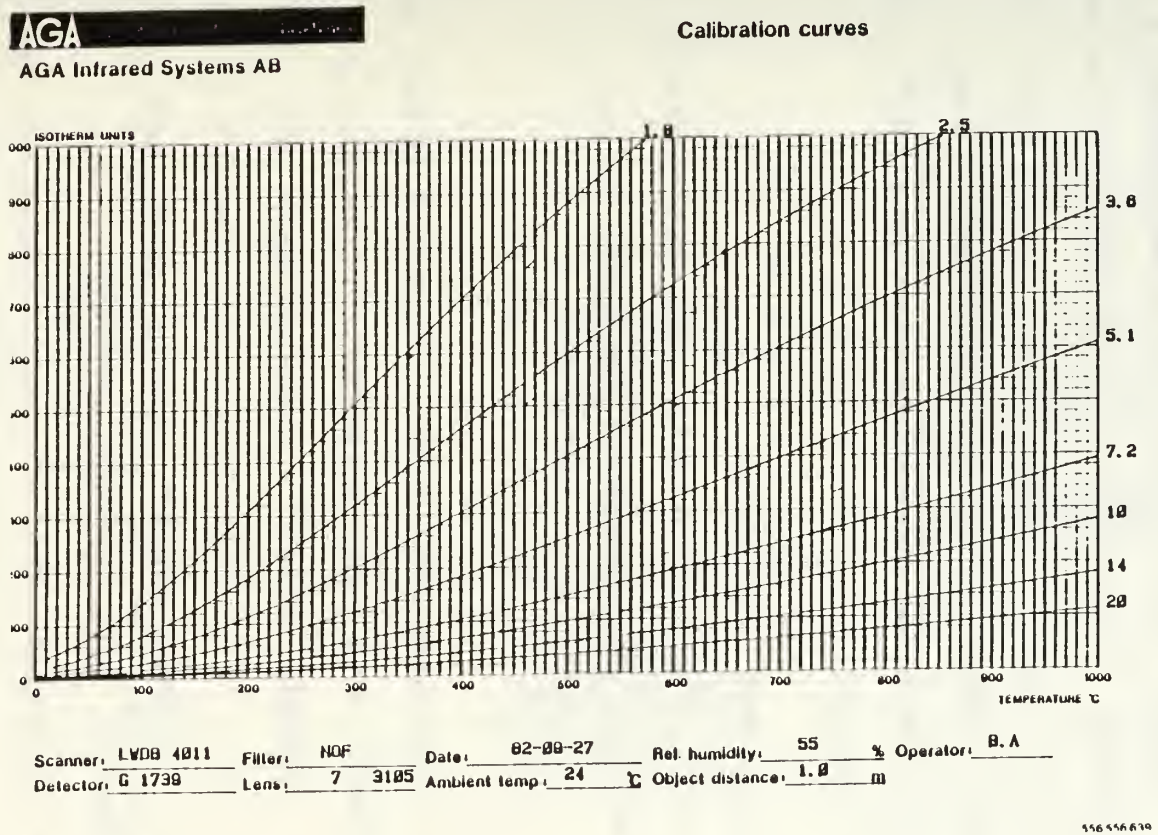

Figure 5.9 : LW calibration curves for the AGA 780. Temperature range from 0°C to 1000°C. [Ref. 7]

received from an external reference source of known temperature and emissivity.

For our purpose the Direct measurement method was used mainly because of the lack of an "ideal reference", ie. an object of known temperature, having the same emissivity and situated near the observed object. For example it was (almost) impossible to have an "ideal reference" near a cloud.

D. DIRECT MEASUREMENT PROCEDURE

Assuming that the emissivity of the object and the transmittance of the atmosphere are equal to one,

$$\epsilon_o = 1$$
$$\tau_a = 1 \qquad \text{(V-1)}$$

the following procedure was used (figure 5.10 and 5.11 show the equipment and the procedure respectively):

(i) The "THERMAL LEVEL" control knob was set to some specific value "L" ,to obtain a satisfactory picture.

(ii) The "THERMAL RANGE" control knob was set to improve the picture obtained above.

(iii) The "ISOTHERM LEVEL 1" control knob was set at some value "i" in order to brighten up the object of interest.

(iiii) The values "L" and "i" were added to obtain the radiance I in Isotherm Units.

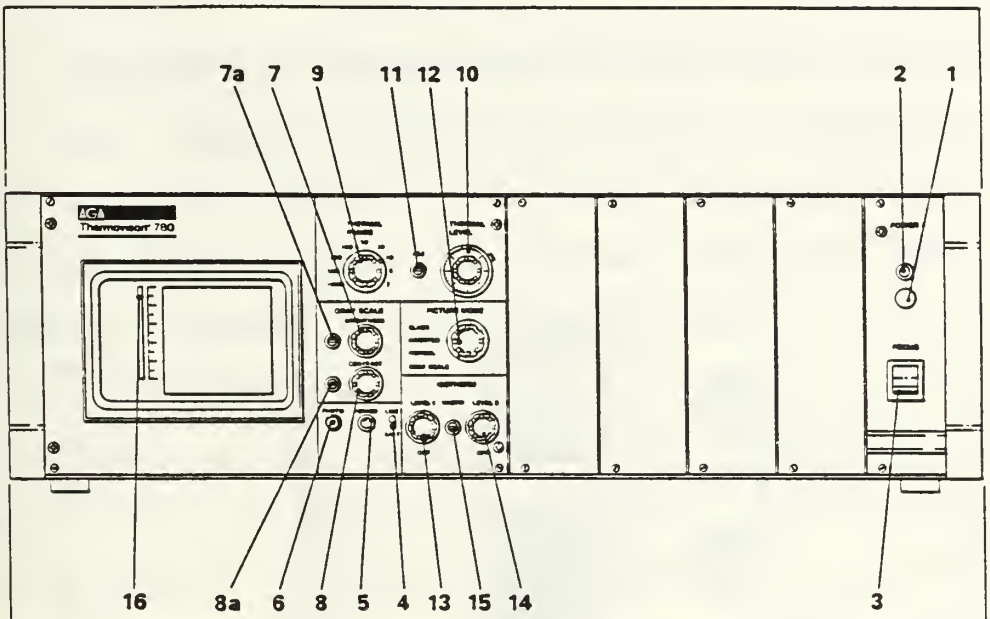

1. POWER
2. LED
3. FOCUS
4. LINE/BATT
5. POWER LED
6. PHOTO
7. BRIGHTNESS
7a. BRIGHTNESS PRESET
8. CONTRAST
8a. CONTRAST PRESET
9. THERMAL RANGE
10. THERMAL LEVEL
11. THERMAL LEVEL ADJ.
12. PICTURE MODE
13. ISOTHERM LEVEL 1
14. ISOTHERM LEVEL 2
15. ISOTHERM WIDTH
16. ISOTHERM SCALE

Figure 5.10 : Front face of the AGA black and white monitor showing the different controls. [Ref. 7]

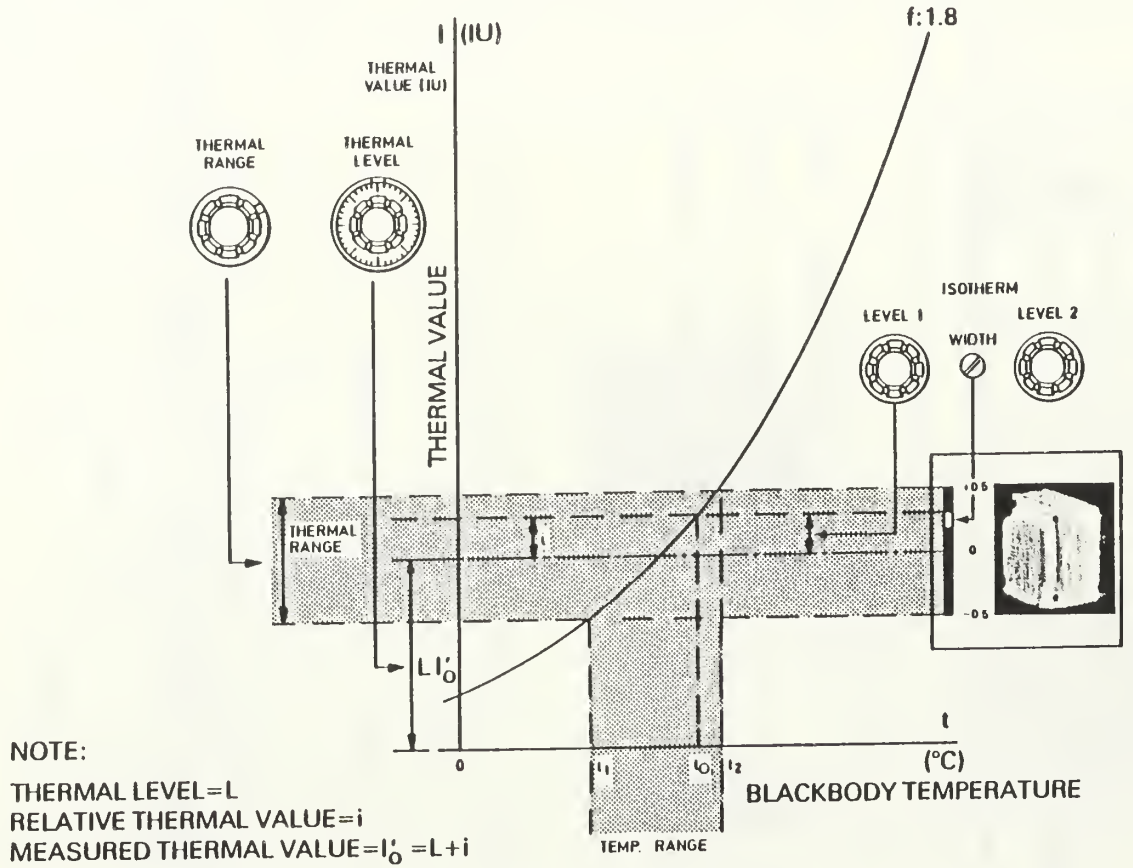

Figure 5.11 : Direct measurement technique. [Ref. 7]

E. CORRECTION OF MEASUREMENTS FOR NON-IDEAL SITUATION

Many factors affect the radiation received by the AGA 780 from an object . The most important ones and the actions taken, either to correct them or just to take them into account , are listed below.

(i) Emissivity.

Most of the objects have an emissivity less than one ($\epsilon < 1$) , often non-uniform over the spectral range ($\epsilon = \epsilon(\lambda) < 1$). Typically the emissivity of a cloud ranges from 0.2 to 0.8 but for clouds of thickness greater than 100 m the emissivity can be assumed to be close to unity. (refer to III-B-3)

(ii) Object reflections

An object will emit not only its own radiation but also it will reflect radiation from other objects (surroundings). If the object to be measured does not transmit IR radiation its reflectivity will be

$$\rho = 1 - \epsilon \qquad (V-2)$$

So , according to the assumption made in the above a cloud's reflectivity will be less than 0.1 .

(iii) Object size

If the object does not cover the solid angle subtense of the detector then radiation will be received from the background. In most of the measurements made here an effort was made to have the object more or less covering the entire field-of-view.

(iiii) Atmospheric absorption

Water vapor or ice (H_2O),Carbon dioxide (CO_2) and also some other constituents of the atmosphere absorb the IR radiation. Thus IR radiation received by the system will be less than that emitted by the object observed. The ratio of these two is the transmittance of the atmosphere , τ_a , and is provided by the LOWTRAN code.

VI. EMPIRICAL CALIBRATION OF THE AGA

A. GENERAL

An empirical calibration of the "AGA Thermovision 780" was made in order to determine if the calibration curves provided by the manufacturer were accurate enough under the circumstances in which the equipment was used.

The calibration of the AGA consisted of a two scale experiment :

(i) A near field experiment and,

(ii) A far field experiment.

B. NEAR FIELD EXPERIMENT

The thermal radiance of an aluminium can filled with water was measured. The can was painted black (painting procedure :1. Aluminium plate polished, 2. first coating , zinc chromate TT-P-1757 , 3. second coating , flat black paint , Part no. 8010 582 5382) in order to have emissivity close to unity, and was placed at a distance of 4 m from the AGA (figure 6.1 shows the setup for the experiment). The water in the can was heated from ambient temperature up to its boiling point. The temperature of the can was measured with a

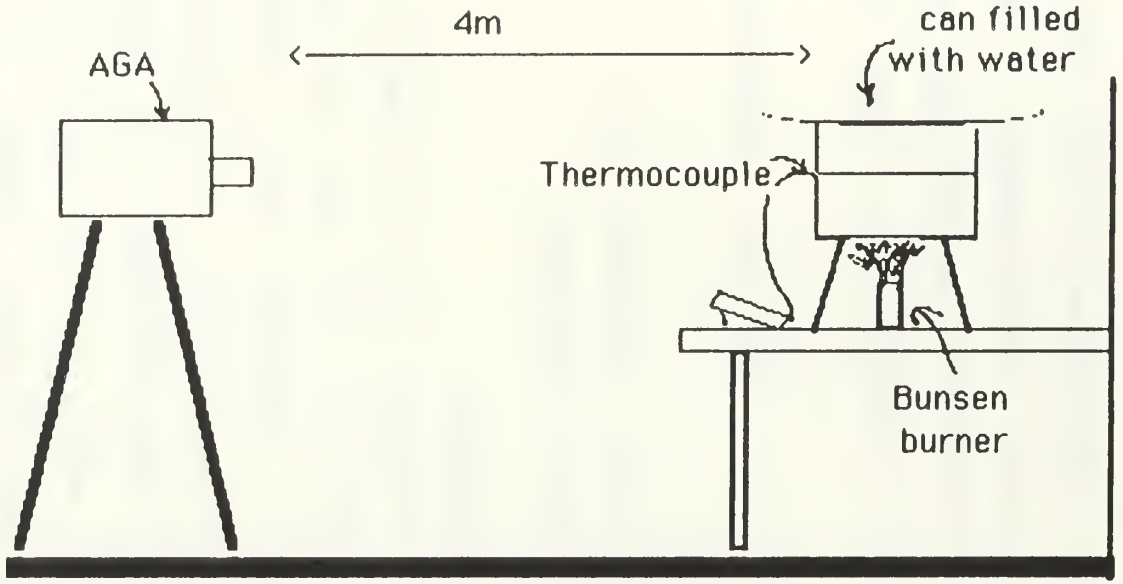

Figure 6.1 : Near field calibration setup.

thermocouple and every 2°C measurements of the thermal radiance were made using the AGA.

This experiment was carried out twice and the "Isotherm Units" reading of the AGA for each temperature appears in Table 2 . In figures 6.2 and 6.3 IU's are plotted versus temperature for SW and LW respectively. In these same figures the calibration curves given by the manufacturer were also plotted for comparison purposes . As can be seen the empirical calibration , data falls pretty well into the manufacturers curves. The data of the curves noted "empirical calibration 2" is a little offset , it is believed , mainly because of inaccuracies in the thermocouple readings of the temperature (offset of approximately 3 to 4°C).

C. FAR FIELD EXPERIMENT

The thermal radiance of an aluminium plate of 1 m^2 surface (1mX1m) was measured. The plate was painted black (Same painting procedure used as the one described for the Aluminium plate) in order to have emissivity close to unity. The experiment was carried out during two periods on the roof of Spanagel Hall (building 232 ,NPS). The plate heated by the sun can be assumed to have small fluctuations in its temperature throughout the experiment. Readings were taken with the plate at

TABLE 2

NEAR FIELD MEASUREMENTS

Temp.(°C)	SW (IU) 1st exp.	SW (IU) 2nd exp.	LW (IU) 1st exp.	LW (IU) 2nd exp.
48	51	-	77	-
50	53	-	79	-
52	57	-	81	-
54	61	-	83	-
56	63	-	85	-
58	66	-	87	-
60	71	77	90	94
62	76	83	92	97
64	80	86	93	99
66	84	90	96	101
68	89	95	98	103
70	96	99	101	105
72	99	104	103	107
74	104	109	106	109
76	106	113	107	110
78	112	122	109	114
80	116	127	111	117
82	121	134	114	120
84	130	139	116	121
86	133	148	119	124
88	142	155	121	126
90	147	165	124	132
92	155	171	127	134
94	-	177	-	136
96	-	183	-	138

Note: Ambient temperature : 23°C

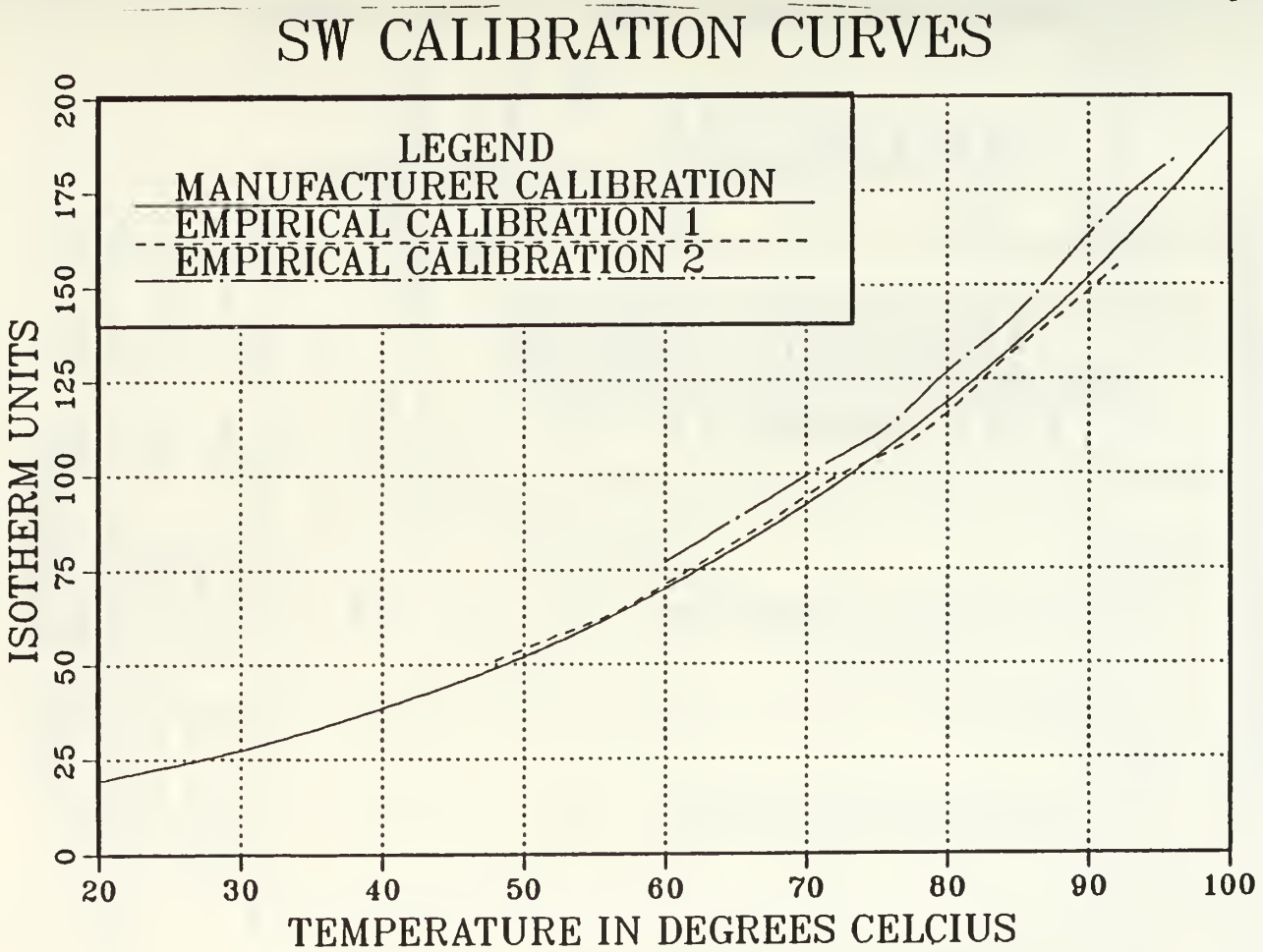

Figure 6.2 : SW calibration curves.

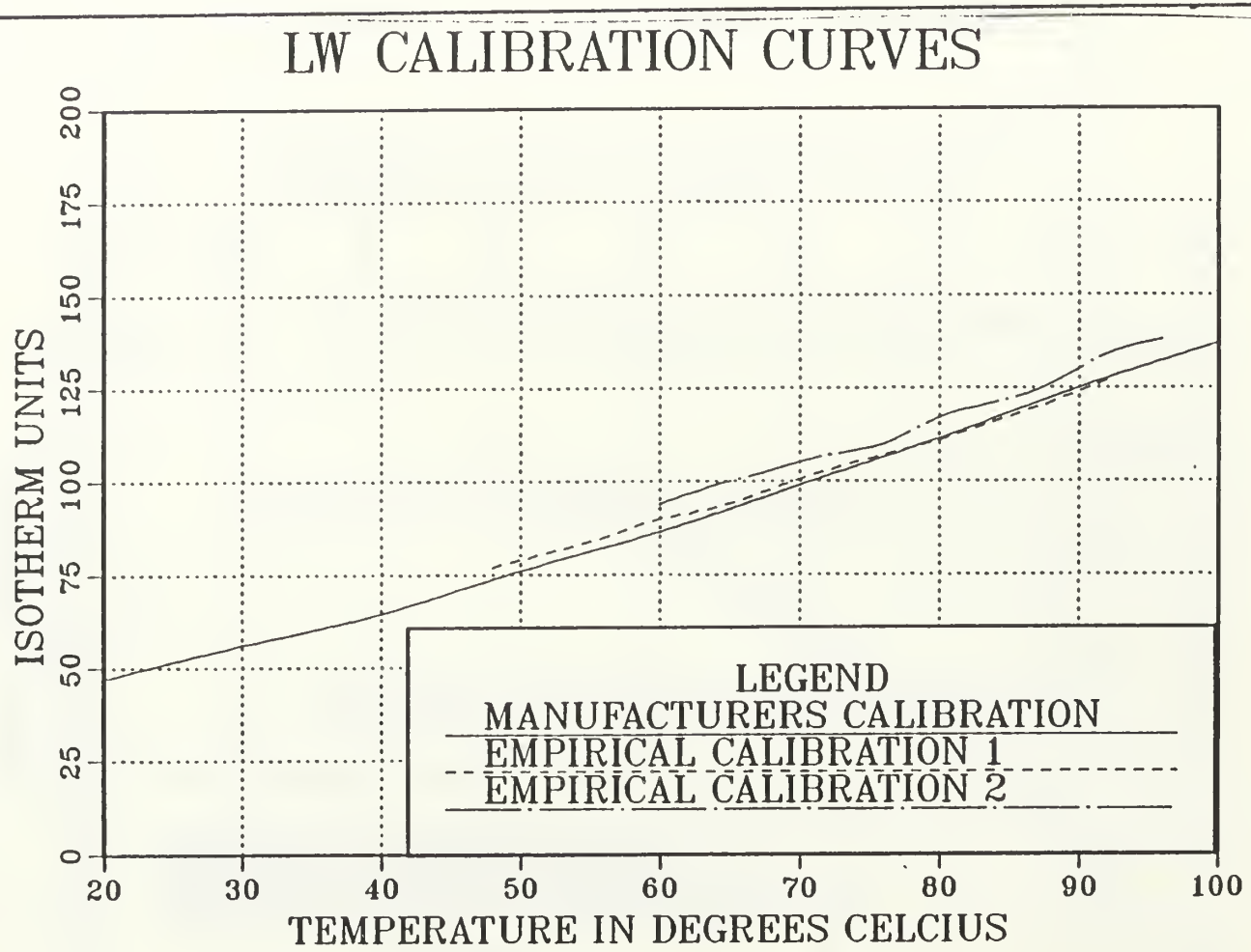

Figure 6.3 : LW calibration curves.

TABLE 3

FAR FIELD MEASUREMENTS

	SW (IU)		LW (IU)	
Distance (ft)	1st exp.	2nd exp.	1st exp.	2nd exp.
30	48	48	76	78
60	48	48	72	78
90	46	47	68	78
120	48	44	75	75
150	47	44	74	75
180	46	44	74	75
210	44	41	74	74
240	**	41	75	73
270	**	39	74	71
300	**	37	74	71
330	**	**	75	72
360	**	**	73	74
390	**	**	71	**
Mean	46.7	43.3	73.5	74
Standard deviation	1.5	3.7	2.1	2.3
Corresponding temperature(°C)	43.5 *	42 *	47 *	47 *

Notes : * The actual temperature of the plate was
in the 1st exp. : 42°C at the center,
37°C at the corners.
in the 2nd exp. : 44°C at the center
38°C at the corners.

** Plate not detectable by the system.

different distance intervals (from the AGA) from 30ft up to 390ft away.

The values obtained appear in Table 3 . These values as it can be seen are more or less the same , independent of distance.

Specifically for the first far field set of measurements the plate temperature was 42° C at the center and 37° C at the corners and the average thermal values measured were 46.7 IU in SW (with standard deviation σ =1.5 IU) and 73.5 IU in LW (with σ =2.1 IU). These values correspond to 43.5 °C in SW and 47 °C in LW.

For the second set of measurements the temperature of the plate was 44° C at the center and 38° C at the corners. The average thermal values measured were 43.3 IU in SW (σ =3.7 IU) and 74 IU in LW (σ =2.3 IU) corresponding to 42° C and 47° C respectively.

D. CONCLUSIONS FROM EMPIRICAL CALIBRATION

The conditions of the experiment (Estimated accuracies : IU reading ± 5% , thermocouple reading ± 5%) were not good enough to give good empirical calibration curves.

The near field experiment showed that empirical calibration curves are not better than manufacturer's

curves and the far field experiment showed that absorption of the atmosphere is not a big factor at small distances (up to 130m).

What has been shown is that for the purpose of the present work one should better use the manufacturer's calibration curves and keep in mind that the results will have a tolerance of at least ±5% (IU reading accuracy).

VII. SIGNATURE MEASUREMENTS

A. MEASURED OBJECTS

All the measurements, using the AGA , were made from the roof of Building 232 (Spanagel Hall) of the Naval Postgraduate School (NPS), (observers height 30m).

The objects measured were in the vicinity of the NPS and specifically the following :

(i) Different cloud formations at different ranges and altitudes.

(ii) The following buildings:

(a) The Monterey Sheraton Hotel located at 401 Alvarado St., Monterey CA. 93940.

(b) Halligan Hall (building 234 of the NPS)

(c) A warehouse located at 1260 9^{th} St., Monterey CA. 93940, viewed across the NPS.

Figure 7.1 is a map of the Naval Postgraduate School showing the location of Halligan Hall and the warehouse at 9^{th} St. and figure 7.2 is a map of the city of Monterey showing the location of the Monterey Sheraton Hotel .

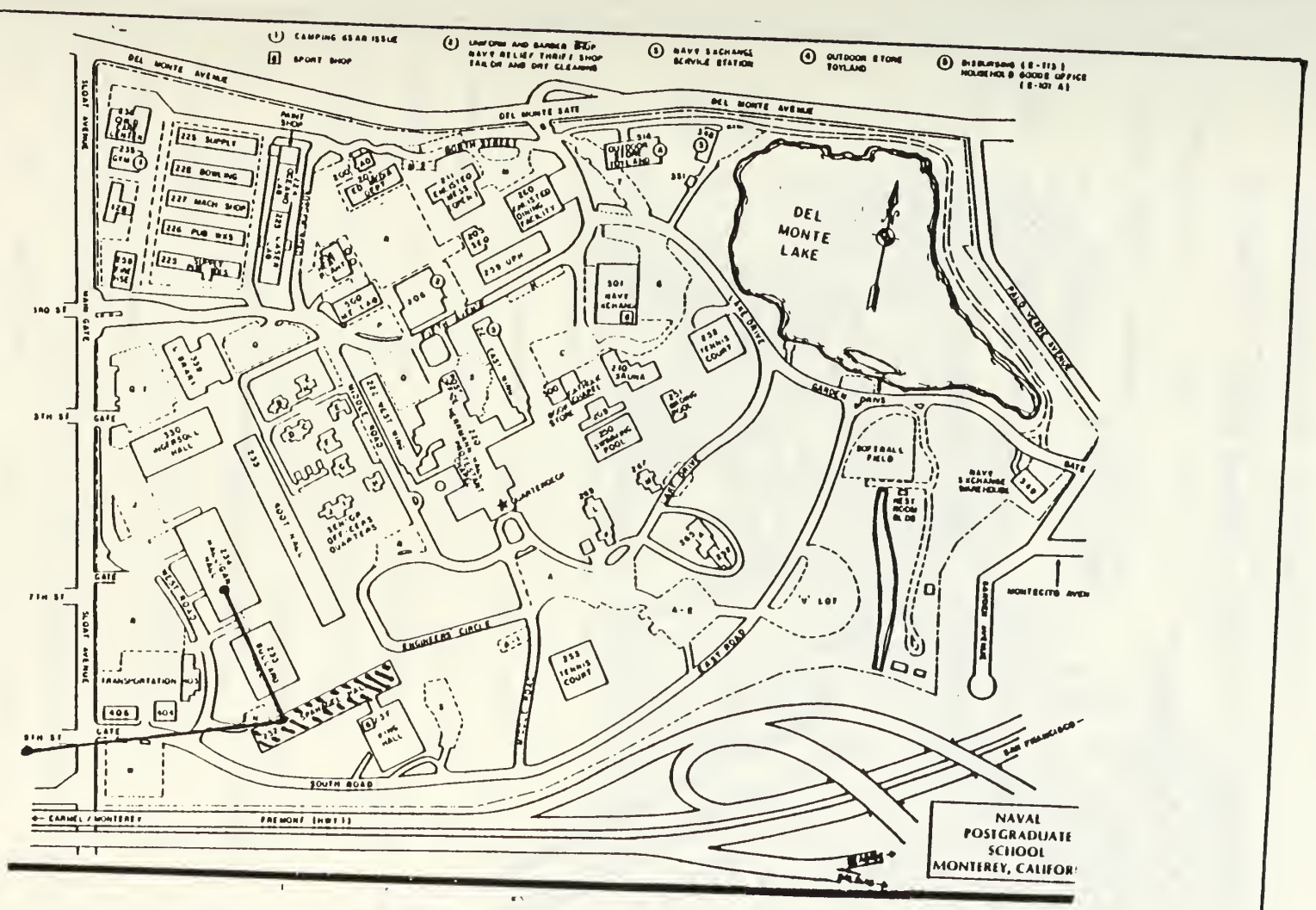

Figure 7.1 : Naval Postgraduate School.

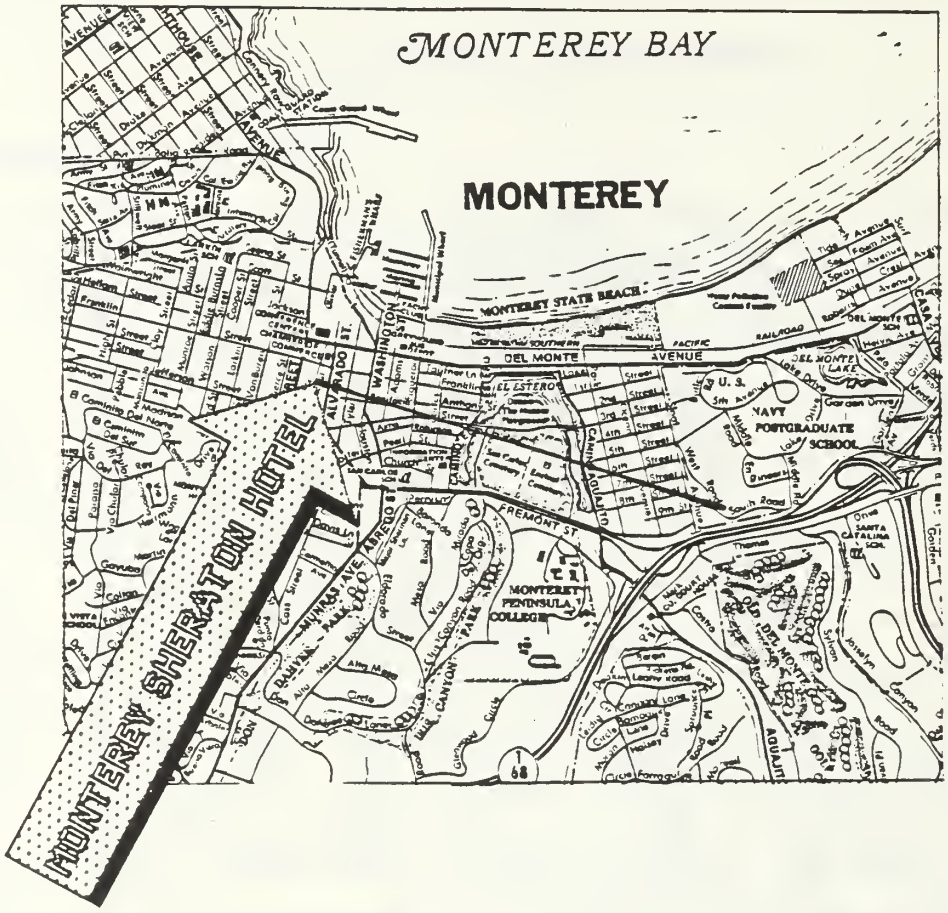

Figure 7.2 : Map of Monterey ,CA.

B. FORMULATION OF MEASUREMENTS

An object will emit thermal radiation due to its temperature. The objective of the present work is to find this thermal radiance.

The radiation received by the AGA is the sum of the object radiation, the radiation reflected by the object and the radiation emitted from the atmosphere (figure 7.3).

If we make two assumptions :

(i) That the observed object is opaque (ie. there is no transmission of IR radiation through the object), and,

(ii) That the ambient temperature is uniform for all surroundings :

we can assume that the three factors above are equivalent to three objects laid one on top of the other , with the same dimensions , that emit photon fluxes S_o , S_a and S_{atm} respectively.

S_o is the photon flux (photons/sec), into the FOV of the receiver , emitted from a blackbody of temperature t_o at short distance, ie. no atmospheric absorption present.

S_a is the photon flux (photons/sec), into the FOV of the receiver , due to reflection of ambient radiation from the object .

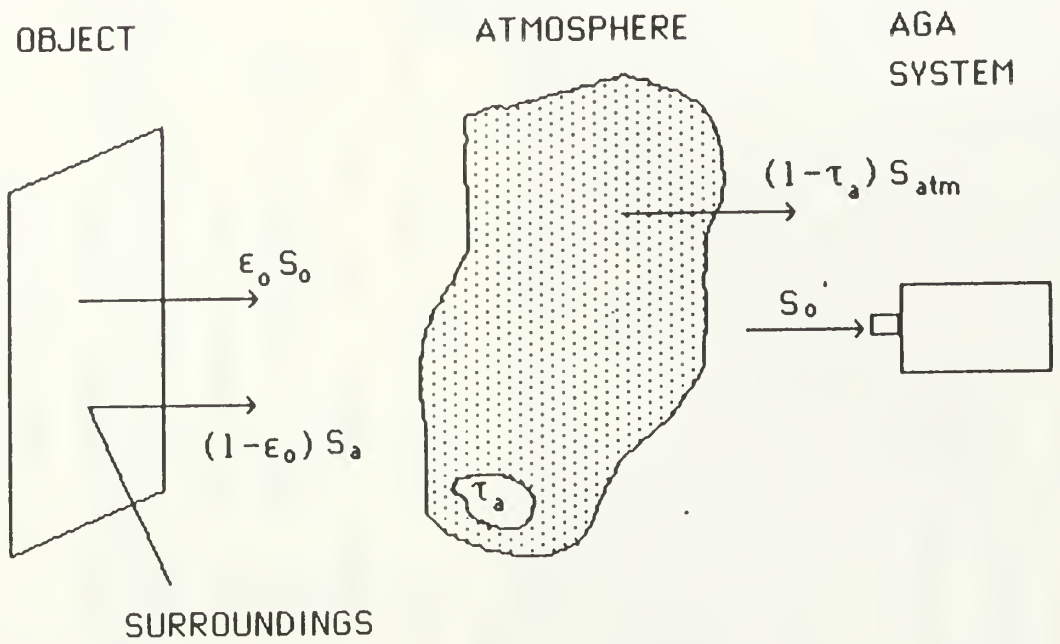

Figure 7.3 : The radiation budget.

S_{atm} is the photon flux (photons/sec) , into the FOV of the receiver , due to atmospheric emission and scattering.

t_o is the object temperature.

The first object , being the source itself , emits photon flux equal to $\epsilon_o S_o$, which attenuated via the atmosphere becomes

$$\text{object radiation} = \epsilon_o \tau_a S_o$$

The second object , corresponding to the radiation reflected by the object , will emit photon flux equal to $\rho_o S_a$, where ρ_o is the reflection coefficient of the source. From the assumption that the source is opaque we have that

$$\rho_o = 1 - \epsilon_o$$

then the reflected photon flux is equal to $(1-\epsilon_o)S_a$ which attenuated through the atmosphere becomes

$$\text{reflected radiation} = \tau_a(1-\epsilon_o)S_a$$

Finally the radiation emitted from the atmosphere will be,

$$\text{atmospheric radiation} = (1-\tau_a)S_{atm}$$

Then we can write the radiation received by the AGA in the form of the following summation

$$S_o' = \tau_a \epsilon_o S_o + \tau_a (1-\epsilon_o) S_a + (1-\tau_a) S_{atm} \qquad \text{(VII-1)}$$

=object radiation

+ reflected radiation

+ atmospheric radiation

where ,

S_o' : is the radiation received via the atmosphere from the object surface (photons/sec).

ϵ_o : is the emissivity of the object .

τ_a : is the atmospheric transmittance .

The "AGA 780" has a linear photon counting detector. Thus the relationship between S values (photons/sec) and thermal values I (IU) is a linear one .

$$I = C \times S$$

where C is a constant factor relating the signal in Isotherm Units to the received photon flux at the receiver (ie. C is an instrument response factor).

This yields ,

$$I_o' = \tau_a \epsilon_o I_o + \tau_a (1-\epsilon_o) I_a + (1-\tau_a) I_{atm} \qquad \text{(VII-2)}$$

where the I values are radiation detected by the AGA in IU and refer to the calibration curves of IU vs T °C provided by the manufacturer .

Equation (VII-2) solved for I_o gives ,

$$I_o = \frac{I_o'}{\epsilon_o \tau_a} - \left(\frac{1}{\epsilon_o} - 1\right) I_a - \frac{1}{\epsilon_o}\left(\frac{1}{\tau_a} - 1\right) I_{atm} \qquad \text{(VII-3)}$$

I_o' is the measured IU (thermal) value and I_o is the thermal value of the object at the position of the object . By thermal value is meant the radiance of the object converted into IU through the calibration curves .

If we assume that the ambient temperature (t_a) is the same as the atmospheric temperature (t_{atm}) then the equivalent source thermal values from the surroundings and the atmospheric path will be equal, and equation (VII-3) can be rewritten as follows,

$$I_o = \frac{I_o'}{\epsilon_o \tau_a} - \left(\frac{1}{\epsilon_o \tau_a} - 1\right) I_a \qquad \text{(VII-4)}$$

$$\text{or, } I_o = \frac{I_o' - I_a}{\epsilon_o \tau_a} + I_a \qquad \text{(VII-5)}$$

Equation (VII-5) will be used to give the source thermal value of the object in IU , and from that the radiance of the object ($W/cm^2 sr$) will be computed.

The procedure that was followed appears in the next section.

C. APPLICATION OF THE FORMULATION TO THE EXPERIMENTAL DATA

(1) A measurement with the AGA will provide a value I_o' (of irradiance equivalence) in IU.

(2) Entering the calibration curves of the AGA with the ambient temperature (t_a) we obtain the value I_a (IU) .

(3) From the LOWTRAN 6 code with the meteorological and geographical data of each case we obtain the transmittance of the atmosphere ,τ_a .

(4) The emissivity will be assumed to be 0.90 for clouds (in the SW) and 0.80 for buildings in the SW). The LW emissivity is calculated assuming the emissivities in the SW are correct , as analyzed in the next chapter.

(5) Using equation (VII-5) we obtain the thermal value I_0 of the object .

(6) From the thermal value I_o of the object we find , using the calibration curves again , its temperature . The temperature of the object calculated from the SW data has been assumed to be the correct one (see Chapter 8).

(7) Using a TI-59 program (listing and analysis of that program appears in Appendix A) we compute the in-band radiant flux density M_0 (W/cm^2) of the object.

(8) If the observed object is a flat lambertian surface then the radiance , L_0 , from that object will be ,

$$L_{0L} = \frac{\epsilon M_0}{\pi} \qquad (W/cm2\ sr) \qquad (VII-6)$$

The lambertian surface assumption was reasonable for most of the objects observed .

For clouds where the thickness is much less than the range of observation another approximation might be considered ; the spherical surface approximation where the radiance of that object will be ,

$$L_{0S} = \frac{\epsilon M_0}{4\pi} \qquad (W/cm2\ sr) \qquad (VII-7)$$

This last approximation was never used because in all the cases observed the extent of the clouds was greater than or about equal to the range of observation.

D. SAMPLE CALCULATION

(1) The radiance of a cloud in the SW and LW windows was measured . The values obtained were 20 and 49 IU respectively.

$$I_{0SW}' = 20 \quad IU$$

$$I_{0LW}' = 49 \quad IU$$

(2) Entering the calibration curves with the ambient temperature t_a = 20°C we obtained the value I_a,

$$I_{aSW} = 19.5 \quad IU$$

$$I_{aLW} = 47.5 \quad IU$$

(3) From the LOWTRAN 6 code we obtained

$$\tau_a = 0.1167 \quad \text{in the SW , and}$$

$$\tau_a = 0.3721 \quad \text{in the LW}$$

(4) Since we dealt with a cloud, its emissivity in the SW was assumed to be 0.90 and the LW emissivity was calculated as 0.733 (this calculation appears in the next chapter).

$$\epsilon_{SW} = 0.9$$

$$\epsilon_{LW} = 0.733$$

(5) Using equation (VII-5) we obtained

$$I_{OSW} = \frac{20-19.5}{0.9X0.1167} + 19.5 \quad IU$$

or, $I_{OSW} = 24.3 \quad IU$

(6) From the calibration curves we found the temperature of the cloud as 26°C using the SW I_o value and 23°C using the LW I_o value . This deviation is attributed to departure of the spectral radiance from the blackbody curve in the vicinity of the peak,

as found by E.E. Bell et al. [Ref. 14]. This "short wave" temperature is thus assumed to be appropriate.

(7) Using the TI-59 program the in-band radiant flux density was computed for the two wavebands.

$$M_{0SW} = 0.001178 \quad W/cm^2$$

$$M_{0LW} = 0.01699 \quad W/cm^2$$

(8) Finally dividing by π and multiplying by the corresponding emissivity we obtained the in-band radiance of the cloud in the SW and the LW windows.

$$L_{0SW} = \frac{\epsilon M_{0SW}}{\pi}$$

or,

$$L_{0SW} = \frac{0.9 \times 0.001178}{\pi} = 3.375 \times 10^{-4} \quad W/cm^2 sr$$

and,

$$L_{0LW} = \frac{\epsilon M_{0LW}}{\pi}$$

or,

$$L_{0LW} = \frac{0.733 \times 0.0165}{\pi} = 3.964 \times 10^{-3} \quad W/cm^2 sr$$

Here the LW radiance is computed using the "long wave" emissivity ϵ_o as computed in Chapter eight.

VIII. DATA ANALYSIS, PRESENTATION OF RESULTS

A. DATA ANALYSIS

1. Emissivity

The major uncertainty in the determination of cloud radiance from direct radiometric measurements is the determination of the appropriate value of emissivity . In the absence of a reference source at or near the location of the cloud this can only be inferred indirectly.

The procedure adopted to determine source temperature was carried out using an assumed value (appropriate to literature values) of 0.9 for both long and short wavebands. In all cases the temperature of the object calculated from the SW data , assuming that the emissivity was 0.90 in both SW and LW (graybody approximation) , was greater than the temperature calculated using the LW data.

An interpretation of this result is clear if we observe figures 3.2 and 3.3 . There we can see that for about the same conditions of measurements as the ones we had (cirrus-cumulus clouds, elevation angle $\approx 15°$) the cloud spectrum approaches the blackbody curves in the 3-5.6 μm range but is far different (less) in the

8-14 μm window . The same was also observed for a city scene in figure 3.16.

This phenomenon is not due to the atmospheric transmittance because as it can be seen in Table 5 the transmittance in the SW is less than that in the LW.

The reasonable interpretation of this is that the emissivity in the SW is close to one (according to figures 3.2 and 3.3) , but that this is not the case in the LW .

To account for this variation the emissivity in the SW has been assumed to be 0.9 for clouds and 0.8 for buildings . Using these values a temperature of the object is deduced . This temperature has been assumed to be correct , and from this tracking back a consistent emissivity for the the LW has been calculated.

The procedure used is described below.

2. Calculation of the emissivity in the LW

Equation (VII-5) solved for ϵ_o yields

$$\epsilon_o = \frac{I_o' - I_a}{\tau_a (I_o - I_a)} \qquad \text{(VIII-1)}$$

In this equation I_o' is the measured thermal value (IU) of the object , I_a is the atmosphere thermal value (IU) , I_o is the object thermal value

taken from the calibration curves where we enter with the temperature of the object as computed with the SW data , and τ_a is the transmittance calculated with the LOWTRAN 6 code.

The following is a sample calculation of the emissivity in the LW band.

In section VII.D the temperature of the cloud using the SW data was calculated to be 26°C.

With this value entering the calibration curves we get,

I_o = 53 IU

The other variables on the right hand side of equation VIII-1 are the same as in section VII.D,

I_o'= 49 IU

I_a = 47.5 IU

τ_a = 0.3721

Equation VIII-1 then gives an emissivity for the LW,

ϵ_{oLW} = 0.733

This emissivity is then used in step VII.D.(8) to calculate the in-band radiance of the cloud in the LW.

3. Comments

In some cases the computed emissivity in the LW did not fall in the permissible range ($0<\epsilon<1$).

This may have been caused by a number of factors, of which the most likely are the following :

(a) Invalid assumption that the emissivity is 0.9 or 0.8 (clouds or buildings) in the SW.

(b) Different transmittance from the one computed by the LOWTRAN 6 code .

(c) Invalid assumption that the objects measured are opaque.

(d) Error in the measurement.

The analysis showed that the emissivity of the clouds in the SW is more or less close to unity; therefore the assumption of their emissivity being .9 should be correct with an estimated error of ± .1 . The same holds for the emissivity of the buildings .

The transmittance computed by the LOWTRAN 6 code might be in error , since the atmospheric model used (Midlatitude Winter) might not match with the actual atmospheric conditions. No local meteorological measurements were made during the experiments. The magnitude of the error inserted in the computation of the emissivity , due to a transmittance error of a factor of 0.3 , will be a factor of three .

The assumption of opacity of the objects is valid for the buildings and for clouds thicker than 60 m (fig. 3.11).

The main source of errors comes from the measurement itself . An accuracy in the measured thermal value I_o' of ± 3 IU (which is about ±6%) could yield an emissivity error of about ± 0.9 which will cause the calculated emissivity to exceed the accepted range, ($0<\epsilon<1$).

For those cases in which the computed emissivity in the LW was outside the valid range it has been assumed to be 0.7 for computation of radiance.

B. PRESENTATION OF RESULTS

The data collected appear in Table 4 along with information about the range of the object. Data on clouds was obtained from Monterey Air Traffic Control Tower (MATCT) and from Fritzsche Field (Fort Ord) .

Table 5 shows the LOWTRAN atmospheric transmittance for each case along with the clear sky radiance.

Table 6 shows the calculated radiance of the different objects along with their emissivity .

Finally the average radiance values obtained appear in Table 7.

TABLE 4

DATA COLLECTED

Number of measurement	Object	Meas. (IU) SW	Meas. (IU) LW	Range
1.	SHERATON	25	52	3.7km
2.	HALLIGAN	26	54	100m
3.	WAREHOUSE	27	54	150m
4.	CLOUD	20	49	10km
5.	SHERATON	20	45	3.7km
6.	CLOUD	16	44	10km
7.	CLOUD	15	42	10km
8.	CLOUD	16	43	15km
9.	CLOUD	15	40	15km
10.	HALLIGAN	25	50	100m
11.	WAREHOUSE	23	50	150m
12.	CLOUD	16	40	10km
13.	CLOUD	16	43	15km
14.	CLOUD	17	42	15km
15.	CLOUD	18	44	10km
16.	CLOUD	15	42	10km
17.	LOW CLOUD	21	44	7km
18.	LOW CLOUD	21	45	7km
19.	CLOUD	16	44	10km

Note: (1) The ambient temperature for measurements 1 through 4 was 20°C , and for measurements 5 through 19 , 14°C.

(2) The range to the clouds was estimated from weather information provided by the Monterey Air Traffic Control Tower (MATCT) on the cloud coverage of the Monterey Bay area.

TABLE 5

LOWTRAN OUTPUT

Number of meas.	Transmittance		Radiance ($W/cm^2 sr$)	
	SW	LW	SW ($X\ 10^{-4}$)	LW ($X\ 10^{-3}$)
1.	0.4296	0.7574	0.9966	0.8437
2.	0.7954	0.9618	0.4997	0.1593
3.	0.7954	0.9618	0.4997	0.1593
4.	0.1167	0.3721	0.944	1.866
5.	0.4296	0.7574	0.9966	0.8437
6.	0.1067	0.4972	1.231	1.547
7.	0.2065	0.5157	1.021	1.497
8.	0.1247	0.3872	0.9753	1.832
9.	0.1247	0.3872	0.9753	1.832
10.	0.7954	0.9618	0.4997	0.1593
11.	0.7954	0.9618	0.4997	0.1593
12.	0.1067	0.4972	1.231	1.547
13.	0.1247	0.3872	0.9753	1.832
14.	0.1247	0.3872	0.9753	1.832
15.	0.1935	0.4972	1.001	1.547
16.	0.1935	0.4972	1.001	1.547
17.	0.2243	0.5403	1.014	1.45
18.	0.2243	0.5403	1.014	1.45
19.	0.1935	0.4972	1.001	1.547

The above values are path average transmittance and path radiance computed using the LOWTRAN 6 code.

TABLE 6

COMPUTED RADIANCE

Number of meas.	SW emiss.	SW Radiance $W/cm^2 sr$ $X10^{-4}$	LW emiss.	LW Radiance $W/cm^2 sr$ $X10^{-3}$
1.	0.8	3.888	0.838	5.108
2.	0.8	3.5345	0.778	4.539
3.	0.8	3.649	0.711	4.210
4.	0.9	3.375	0.733	3.964
5.	0.8	3.476	0.985	5.703
6.	0.9	2.951	0.7 **	3.558
7.	0.9	1.928	0.7 ***	2.923
8.	0.9	2.851	0.32	1.601
9.	0.9	1.791	0.7 ***	2.825
10.	0.8	3.769	0.601	3.612
11.	0.8	3.206	0.742	4.138
12.	0.9	2.951	0.7 **	3.558
13.	0.9	2.851	1	5.004
14.	0.9	3.879	0.49	2.823
15.	0.9	4.105	0.7 **	4.144
16.	0.9	1.859	1	4.107
17.	0.9	5.767	0.22	1.525
18.	0.9	5.767	0.516	3.576
19.	0.9	2.851	1	5.004

The emissivity in the SW band is assumed as 0.9 for clouds and 0.8 for buildings .

The emissivities marked ** or *** are assumed 0.7 because the calculation yielded emissivity out of accepted limits (>1 and <0 respectively)

TABLE 7

AVERAGE RADIANCE VALUES

	SW RADIANCE $W/cm^2sr \times 10^{-4}$	LW RADIANCE $W/cm^2sr \times 10^{-3}$
CLOUD FORMATIONS	3.302	3.544
MONTEREY SHERATON	3.682	5.406
HALLIGAN HALL	3.652	4.076
WAREHOUSE AT 9th ST.	3.428	4.174

IX. CONCLUSIONS / RECOMMENDATIONS

A. CONCLUSIONS

The radiance measurements obtained appear analytically in chapter 8.

A comparison of radiance from a cloud, for example, and the radiance of the background sky, shows that the cloud would always have, in these cases , a positive contrast with respect to its background. This shows the necessity of the existence of more than a background supression scheme ie. a system that, after the subtraction of the background radiance, will differentiate between real targets and clutter.

B. RECOMMENDATIONS

During the present work the main problem encountered was the translation of IU into meaningful radiance values. The problem was solved by using very general approximations ; the Lambertian surface approximation and the spherical surface approximation.

For better results a calibration curve of IU versus radiance units would be useful. The representative of the AGA Corporation (Mr. Jack M. Patterson , 108 Arena st. , El Segundo , CA. 90245 , tel. (213)- 3226257) has been contacted on that subject

and a telex has been sent to the manufacturing company in Sweden.

At the time of completion of this work no answer yet has been received on the matter.

It is recommended that this subject be pursued because, for any application, and specifically for radiance measurements like the ones made here , it will be very helpful to have on hand a calibration of IU measured versus radiance (W/m^2sr) emitted by an object.

An interesting experiment will be to measure simultaneously an object with both the AGA and the IRSTD and obtain IRSTD signal calibration versus radiance.

APPENDIX A

TI-59 PROGRAM FOR CALCULATION OF THE IN-BAND FLUX

A. GENERAL

The TI-59 program used to calculate in-band flux was originally written by Robert Pitlak (Appollo Lasers, 6357 Arizona Circle , Los Angeles CA 90045) for an HP-67 calculator.

The inputs of the program are:

(1) The initial and final wavelengths that define the band .

(2) The temperature of the object (in °K, or in °C, or in °F).

(3) The number of intervals in the numerical integration (this no. must be even).

The result may be given either in Photons/cm^2 sec or in W/cm^2 .

B. THEORY

Plank's blackbody radiation law may be written in the form:

$$Q = \int_{\lambda_1}^{\lambda_2} c_o \, q \, d\lambda \qquad \text{photons/cm2 sec}$$

$$\text{or,} \quad W = \int_{\lambda_1}^{\lambda_2} c_1 \, (q/\lambda) \, d\lambda \qquad \text{Watts/cm2}$$

where $q = \frac{1}{\lambda^4 (e^x - 1)}$, $x = \frac{c_2}{\lambda T}$

and $c_o = 1.883651556 \times 10^{23}$

$c_1 = 37418.42875$

$c_2 = 14388.32334$

The above integrations are carried out by the TI-59 numerically in any (even) no. of intervals specified by the user.

C. PROCEDURE

To use the program

(1) Load the card into the TI-59 (both faces to be read).

(2) Press RST.

(3) Enter λ_1 in microns , then press R/S.

(4) Enter λ_2 in microns , then press R/S.

(5) Enter T (temperature) then press

A if in °K

B if in °F

C if in °C

(6) Enter n : number of intervals of the numerical integration.

(n MUST be EVEN)

(7) Press D for answer in W/cm^2 .

or E for answer in Photons/sec cm^2 .

D. LISTING OF THE PROGRAM

A listing of the program follows :

```
000  42 STO
001  01  01
002  99 PRT
003  91 R/S
004  42 STO
005  02  02
006  99 PRT
007  91 R/S
008  76 LBL
009  11  A
010  42 STO
011  00  00
012  02  2
013  06  6
014  00  0
015  00  0
016  00  0
017  00  0
018  69 OP
019  04  04
020  43 RCL
021  00  00
022  69 OP
023  06  06
024  69 OP
025  00  00
026  91 R/S
027  76 LBL
028  12  B
029  42 STO
030  00  00
031  02  2
032  01  1
033  00  0
034  00  0
035  00  0
036  00  0
037  69 OP
038  04  04
039  43 RCL
040  00  00
041  69 OP
042  06  06
043  69 OP
044  00  00
045  75  -
046  03  3
047  02  2
048  95  =
049  65  ×
050  05  5
051  55  ÷
052  09  9
053  85  +
054  02  2
055  07  7
056  03  3
057  95  =
058  42 STO
059  00  00
060  91 R/S
061  76 LBL
062  13  C
063  42 STO
064  00  00
065  01  1
066  05  5
067  00  0
068  00  0
069  00  0
070  00  0
071  69 OP
072  04  04
073  43 RCL
074  00  00
075  69 OP
076  06  06
077  69 OP
078  00  00
079  43 RCL
080  00  00
081  85  +
082  02  2
083  07  7
084  03  3
085  95  =
086  42 STO
087  00  00
088  91 R/S
089  76 LBL
090  16  A'
091  42 STO
092  07  07
093  53  (
094  53  (
095  43 RCL
096  07  07
097  45 Y^x
098  43 RCL
099  09  09
100  65  ×
101  53  (
102  53  (
103  43 RCL
104  06  06
105  45 Y^x
106  53  (
107  01  1
108  04  4
109  03  3
110  08  8
111  08  8
112  93  .
113  03  3
114  02  2
115  03  3
116  03  3
117  04  4
118  55  ÷
119  43 RCL
120  07  07
121  55  ÷
122  43 RCL
123  00  00
124  54  )
125  54  )
126  75  -
127  01  1
128  54  )
129  54  )
130  35 1/x
131  65  ×
132  43 RCL
133  08  08
134  54  )
135  92 RTN
136  76 LBL
137  14  D
138  98 ADV
139  42 STO
140  05  05
141  99 PRT
142  98 ADV
143  53  (
144  43 RCL
145  02  02
146  75  -
147  43 RCL
148  01  01
149  54  )
150  55  ÷
151  43 RCL
152  05  05
153  95  =
154  42 STO
155  03  03
156  03  3
157  93  .
158  07  7
159  04  4
160  01  1
161  05  5
162  00  0
163  07  7
164  04  4
165  52 EE
166  04  4
167  42 STO
168  08  08
169  05  5
170  42 STO
171  09  09
172  01  1
173  22 INV
174  23 LNX
175  42 STO
176  06  06
177  36 PGM
178  09  09
179  14  D
180  22 INV
181  52 EE
182  99 PRT
183  98 ADV
184  91 R/S
185  76 LBL
186  15  E
187  98 ADV
188  42 STO
189  05  05
190  99 PRT
191  98 ADV
192  53  (
193  43 RCL
194  02  02
195  75  -
196  43 RCL
197  01  01
198  54  )
199  55  ÷
200  43 RCL
201  05  05
202  95  =
203  42 STO
204  03  03
205  01  1
206  93  .
207  08  8
208  08  8
209  03  3
210  06  6
211  05  5
212  01  1
213  06  6
214  52 EE
215  02  2
216  03  3
217  42 STO
218  08  08
219  04  4
220  42 STO
221  09  09
222  01  1
223  22 INV
224  23 LNX
225  42 STO
226  06  06
227  36 PGM
228  09  09
229  14  D
230  22 INV
231  52 EE
232  99 PRT
233  98 ADV
234  91 R/S
```

LIST OF REFERENCES

1. McCartney, Earl J., Optics of the Atmosphere pp.303-318, John Wiley & Sons Inc., 1976.

2. Lloyd, J.M., Thermal Imaging Systems, pp.18-66, Plenum Press, 1975.

3. Hudson, Richard Jr, Infrared System Engineering, pp.1-60, 104-109, 557, John Wiley & Sons Inc., 1969.

4. Hecht and Zajac , Optics , p.240, Addison-Wesley Publishing Company, 1979.

5. Feigel'son, E.M., Radiation in a Cloudy Atmosphere, pp. 4, 221, 224, 225, D.Reidel Publishing Co.

6. Wolf, William L. and Zissis, George J. , The Infrared Handbook, pp. 3-43 to 3-109, Office of Naval Research, Department of the Navy, 1978.

7. The AGA Thermovision 780 Operating Manual, Aga Co.

8. Kneizys, F.X., and others, Atmospheric Transmittance/ Radiance Computer Code LOWTRAN 6 , Air Force Geophysics Laboratory, AFGL-TR-83-0187, 1983.

9. RCA Electro-Optics Handbook, pp.81-97, RCA Corporation, 1974.

10. Feigel'son, E.M. , Light and Heat Radiation in Stratus Clouds, US Dept. of Commerce and National Science Foundation, 1966.

11. Hobbs, Petter V. and Deepak, Adarsh , Clouds , their Formation , Optical Properties and Effects, Academic Press, 1981.

12. PH 3952 - PH 4952 class notes, Cooper, A.W. and Crittenden ,Naval Postgraduate School.

13. Due, Christopher T., Optical-Mechanical ,Active/Passive Imaging Systems - Volume II , ERIM and Office of Naval Research - Department of the Navy, T53200-2-T II, 1982.

14. Bell, E.E., Eisner, L., Young, J., and Oetjen, R.A., "Spectral Radiance of Sky and Terrain at Wavelengths between 1 and 20 microns. II Sky Measurements", Journal of the Optical Society of America, Vol. 50, December 1960 , pp. 1313-1320.

INITIAL DISTRIBUTION LIST

	No. of copies
1. Defence Technical Information Center Cameron Station Alexandria , Virginia 22304-6145	2
2. Library , Code 0142 Naval Postgraduate School Monterey , CA 93943-5100	2
3. Department Chairman , Code 61 Department of Physics Naval Postgraduate School Monterey , CA 93943	1
4. Prof. A.W. Cooper , Code 61 Cr Department of Physics Naval Postgraduate School Monterey , CA 93943	2
5. Prof. E.C. Crittenden , Code 61 Ct Department of Physics Naval Postgraduate School Monterey , CA 93943	1
6. Department of the Navy SPACE AND NAVAL WARFARE SYSTEMS COMMAND PDW 107-3 Attn: CDR Carver Washington, DC 20363-5100	1
7. Hellenik Navy General Staff GEN / B2 Stratopedon Papagou Holargos - Athens - GREECE	4
8. Alexander Manolopoulos Chrysanthemon 29 P. Psychiko Athens 15452 - GREECE	6

216735

Thesis
M314 Manolopoulos
c.1 Infrared background
and target measurement.